

RECEIVED: February 19, 2016

REVISED: May 6, 2016

ACCEPTED: May 17, 2016

PUBLISHED: June 1, 2016

# Long-range contributions to double beta decay revisited

---

J.C. Helo,<sup>a,b</sup> M. Hirsch<sup>c</sup> and T. Ota<sup>d</sup>

<sup>a</sup> *Universidad Técnica Federico Santa María, Centro-Científico-Tecnológico de Valparaíso, Casilla 110-V, Valparaíso, Chile*

<sup>b</sup> *Departamento de Física, Facultad de Ciencias, Universidad de La Serena, Avenida Cisternas 1200, La Serena, Chile*

<sup>c</sup> *HEP Group, Instituto de Física Corpuscular, C.S.I.C./Universitat de València Edificio Institutos de Investigacion, Parc Científic de Paterna, Apartado 22085, E-46071 València, Spain*

<sup>d</sup> *Department of Physics, Saitama University, Shimo-Okubo 255, 338-8570 Saitama-Sakura, Japan*

*E-mail:* [juancarlos.helo@usm.cl](mailto:juancarlos.helo@usm.cl), [mahirsch@ific.uv.es](mailto:mahirsch@ific.uv.es), [toshi@mail.saitama-u.ac.jp](mailto:toshi@mail.saitama-u.ac.jp)

**ABSTRACT:** We discuss the systematic decomposition of all dimension-7 ( $d = 7$ ) lepton number violating operators. These  $d = 7$  operators produce momentum enhanced contributions to the long-range part of the  $0\nu\beta\beta$  decay amplitude and thus are severely constrained by existing half-life limits. In our list of possible models one can find contributions to the long-range amplitude discussed previously in the literature, such as the left-right symmetric model or scalar leptoquarks, as well as some new models not considered before. The  $d = 7$  operators generate Majorana neutrino mass terms either at tree-level, 1-loop or 2-loop level. We systematically compare constraints derived from the mass mechanism to those derived from the long-range  $0\nu\beta\beta$  decay amplitude and classify our list of models accordingly. We also study one particular example decomposition, which produces neutrino masses at 2-loop level, can fit oscillation data and yields a large contribution to the long-range  $0\nu\beta\beta$  decay amplitude, in some detail.

**KEYWORDS:** Beyond Standard Model, Neutrino Physics

**ARXIV EPRINT:** [1602.03362](https://arxiv.org/abs/1602.03362)

---

## Contents

<b>1</b>	<b>Introduction</b>	<b>1</b>
<b>2</b>	<b>General setup</b>	<b>3</b>
<b>3</b>	<b>Classification</b>	<b>6</b>
3.1	Tree level	6
3.2	One-loop level	8
3.3	Two-loop level	10
<b>4</b>	<b>Left-right symmetric model: <math>d = 7</math> versus <math>d = 9</math> operator</b>	<b>17</b>
<b>5</b>	<b>Summary</b>	<b>19</b>
<b>A</b>	<b>Decompositions of the long range <math>0\nu\beta\beta</math> operators</b>	<b>20</b>

---

## 1 Introduction

Majorana neutrino masses, lepton number violation and neutrinoless double beta decay ( $0\nu\beta\beta$ ) are intimately related. It is therefore not surprising that many models contributing to  $0\nu\beta\beta$  have been discussed in the literature, see for example the recent reviews [1, 2]. However, the famous black-box theorem [3] guarantees only that — if  $0\nu\beta\beta$  decay is observed — Majorana neutrino masses must appear at the 4-loop level, which is much too small [4] to explain current oscillation data [5]. Thus, a priori one does not know whether some “exotic” contribution or the mass mechanism dominates the  $0\nu\beta\beta$  decay rate. Distinguishing the different contributions would not only be an important step towards determining the origin of neutrino masses, but would also have profound implications for leptogenesis [6–8].

In terms of only standard model (SM) fields,  $\Delta L = 2$  terms can be written as non-renormalizable operators (NROs) of odd mass dimensions. At mass dimension  $d = 5$ , there is only one such operator, the famous Weinberg operator [9],  $\mathcal{O}_W = \frac{1}{\Lambda}(LLHH)$ . At tree-level the Weinberg operator can be understood as the low-energy limit of one of the three possible seesaw realizations [10–14]. All other  $\Delta L = 2$  operators up to  $d = 11$  — excluding, however, possible operators containing derivatives — have been listed in [15]. When complemented with SM Yukawa interactions (and in some cases SM charged current interactions), these higher dimensional operators always also generate Majorana neutrino masses (at different loop-levels), leading again to the Weinberg operator<sup>1</sup> at low energies.

All  $\Delta L = 2$  operators also contribute to  $0\nu\beta\beta$  decay. From the nuclear point of view, the amplitude for  $0\nu\beta\beta$  decay contains two parts: the long-range part and the short-range

---

<sup>1</sup>Or to operators of the form  $\mathcal{O}_W \times (H^\dagger H)^n$ ,  $n = 1, 2, \dots$ . For neutrino mass models based on this type of effective operators, see e.g., [16–23].

part. The so-called long-range part [24] describes all contributions involving the exchange of a light, virtual neutrino between two nucleons. This category contains the mass mechanism, i.e. the Weinberg operator sandwiched between two SM charged current interactions, and also contributions due to  $d = 7$  lepton number violating operators.<sup>2</sup> The short-range part of the  $0\nu\beta\beta$  decay amplitude [25], on the other hand, contains all contributions from the exchange of heavy particles and can be described by a certain subset of the  $d = 9$   $\Delta L = 2$  operators in the list of [15]. In total there are six  $d = 9$  operators contributing to the short-range part of the amplitude at tree-level and the complete decomposition for the (scalar induced) operators has been given in [26]. The relation of all these decompositions with neutrino mass models has been studied recently in [27].<sup>3</sup> The general conclusion of [27] is that for 2-loop and 3-loop neutrino mass models, the short-range part of the amplitude could be as important as the mass mechanism, while for tree-level and 1-loop models one expects that the mass mechanism gives the dominant contribution to  $0\nu\beta\beta$  decay.<sup>4</sup>

In this paper we study  $d = 7$   $\Delta L = 2$  operators, their relation to neutrino masses and the long-range part of the  $0\nu\beta\beta$  decay amplitude. We decompose all  $d = 7$   $\Delta L = 2$  operators and determine the level of perturbation theory, at which the different decompositions (or “proto-models”) will generate neutrino masses. Tree-level, 1-loop and 2-loop neutrino mass models are found in the list of the decompositions. We then compare the contribution from the mass mechanism to the  $0\nu\beta\beta$  decay amplitude with the long-range  $d = 7$  contribution. Depending on which particular *nuclear* operator is generated, limits on the new physics scale  $\Lambda \gtrsim g_{\text{eff}}(17 - 180)$  TeV can be derived from the  $d = 7$  contribution. Here,  $g_{\text{eff}}$  is the mean of the couplings entering the (decomposed)  $d = 7$  operator. This should be compared to limits of the order of roughly  $\Lambda \gtrsim \sqrt{Y_{\text{eff}}} 10^{11}$  TeV and  $\Lambda \gtrsim Y_{\text{eff}}^2 50$  TeV, derived from the upper limit on  $\langle m_\nu \rangle$  for tree-level and 2-loop ( $d = 7$ ) neutrino masses. (Here,  $Y_{\text{eff}}$  is again some mean of couplings entering the neutrino mass diagram. We use a different symbol, to remind that  $Y_{\text{eff}}$  is not necessarily the same combination of couplings as  $g_{\text{eff}}$ .) Thus, only for a certain, well-defined subset of models can the contribution from the long-range amplitude be expected to be similar to or dominate over the mass mechanism. Note that, conversely a sub-dominant contribution to the long-range amplitude always exists also in all models with mass mechanism dominance.

We then give the complete classification of all models contributing to the  $d = 7$  operators in tabular form in the appendix of this paper. In this list all models giving long-range contributions to  $0\nu\beta\beta$  decay can be found, such as, for example, supersymmetric models with R-parity violation [34, 35] or scalar leptoquarks [36]. There are also models with non-SM vectors, which could fit into models with extended gauge sectors, such as the left-right symmetric model [37–39]. And, finally, there are new models in this list, not considered in the literature previously. In particular, we have found contributions with

<sup>2</sup>We save the term “long-range contribution” for the contribution from the  $d = 7$  operators and call the standard contribution from Majorana neutrino mass separately the “mass mechanism”.

<sup>3</sup>Neutrino mass models based on the  $\Delta L = 2$  effective operators were discussed in [15, 28] The decomposition of the  $\Delta L = 2$  operators was also discussed in [29, 30].

<sup>4</sup>Possible LHC constraints on short-range operators contributing to  $0\nu\beta\beta$  decay have been discussed in [31, 32] See also [33].

coloured vector-like fermions and exotic coloured vectors, for more details see tables 4 and 5 in the appendix.

We mention that our paper has some overlap with the recent work [40]. The authors of this paper also studied  $d = 7$   $\Delta L = 2$  operators. They discuss 1-loop neutrino masses induced by these operators, lepton flavour violating decays and, in particular, LHC phenomenology for one example operator in detail. The main differences between our work and theirs is that we (a) focus here on the relation of these operators with the long-range amplitude of  $0\nu\beta\beta$  decay, which was not studied in [40] and (b) also discuss tree-level and 2-loop neutrino mass models. In particular, we find that 2-loop neutrino mass models are particularly interesting, because the  $d = 7$  long-range contribution dominates  $0\nu\beta\beta$  only in the class of models. Our study also has some relation to [41, 42]. The  $d = 7$  operators (including the operators with derivatives) are fully listed in [41], and their decomposition and collider phenomenology are discussed in [42]. However, they do not discuss the relation between the lepton number violating operators, double beta decay and neutrino mass models, which we focus on.

The rest of this paper is organized as follows. In the next section we lay the basis for the discussion, establishing the notation and recalling the main definitions for  $\Delta L = 2$  operators and  $0\nu\beta\beta$  decay amplitude. In the following section we then discuss an example of each: tree-level, 1-loop and 2-loop neutrino mass models. In each case we estimate the contribution to the mass mechanism and the constraints from the long-range amplitude. We study a 2-loop  $d = 7$  model in some more detail, comparing also to oscillation data and discuss the constraint from lepton flavour violating processes. In section 4 we then discuss a special case, where a  $d = 9$  operator can give an equally important contribution to the  $0\nu\beta\beta$  decay amplitude as a  $d = 7$  operator. The example we discuss is related to the left-right symmetric extension of the standard model and, thus, of particular interest. We then close the paper with a short summary. The complete list of decompositions for  $d = 7$  operators is given as an appendix.

## 2 General setup

The  $0\nu\beta\beta$  decay amplitude can be separated into two pieces: (a) the long-range part [24], including the well-known mass mechanism, and (b) the short-range part [25] of the decay rate describing heavy particle exchange. Here, we will concentrate exclusively on the long-range part of the amplitude.

The long-range part of the amplitude exchanges a light, virtual neutrino between two point-like vertices. The numerator of the neutrino propagator involves two pieces,  $(m_{\nu_i} + \not{p})$ . If the interaction vertices contain standard model charged current interactions, the  $m_{\nu_i}$ -term is projected out. This yields the “mass mechanism” of  $0\nu\beta\beta$  decay. However, if one of the two vertices involved in the diagram produces a neutrino in the wrong helicity state, i.e.  $(\nu_L)^c$ , the  $\not{p}$ -term is picked from the propagator. Since the momentum of the virtual neutrino is typically of the order of the Fermi momentum of the nucleons,  $p_F \simeq 100$  MeV, the  $0\nu\beta\beta$  amplitude from the operators proportional to  $\not{p}$  is enhanced by  $p_F/m_\nu \gtrsim \mathcal{O}(10^8)$  with respect to the amplitude of the standard mass mechanism. Consequently, any operator

Isotope	$ \epsilon_{V-A}^{V+A} $	$ \epsilon_{V+A}^{V+A} $	$ \epsilon_{S-P}^{S+P} $	$ \epsilon_{S+P}^{S+P} $	$ \epsilon_{TL}^{TR} $	$ \epsilon_{TR}^{TR} $
$^{136}\text{Xe}$	$2.0 \cdot 10^{-9}$	$3.9 \cdot 10^{-7}$	$4.7 \cdot 10^{-9}$	$4.7 \cdot 10^{-9}$	$3.3 \cdot 10^{-10}$	$5.6 \cdot 10^{-10}$

**Table 1.** Limits on  $\epsilon_{\alpha}^{\beta R}$  from non-observation of  $^{136}\text{Xe}$   $0\nu\beta\beta$  decay, where  $\beta_R \in \{S+P, V+A, TR\}$ . These limits were derived in [1] and have been updated with the combined limit from KamLAND-Zen and Exo-200 [46].

proportional to  $\not{p}$  will be tightly constrained from non-observation of double beta decay. Following [24] we write the effective Lagrangian for 4-fermion interactions as

$$\mathcal{L}^{4\text{-Fermi}} = \mathcal{L}^{\text{SM}} + \mathcal{L}^{\text{LNV}} = \frac{G_F}{\sqrt{2}} \left[ j_{V-A}^{\mu} J_{V-A, \mu} + \sum_{\alpha, \beta \neq V-A} \epsilon_{\alpha}^{\beta} j_{\beta} J_{\alpha} \right]. \quad (2.1)$$

The leptonic (hadronic) currents  $j_{\beta}$  ( $J_{\alpha}$ ) are defined as:

$$\begin{aligned} J_{V\pm A}^{\mu} &= (J_{R/L})^{\mu} \equiv \bar{u}\gamma^{\mu}(1 \pm \gamma_5)d, & j_{V\pm A}^{\mu} &\equiv \bar{e}\gamma^{\mu}(1 \pm \gamma_5)\nu, \\ J_{S\pm P} &= J_{R/L} \equiv \bar{u}(1 \pm \gamma_5)d, & j_{S\pm P} &\equiv \bar{e}(1 \pm \gamma_5)\nu, \\ J_{T_{R/L}}^{\mu\nu} &= (J_{R/L})^{\mu\nu} \equiv \bar{u}\gamma^{\mu\nu}(1 \pm \gamma_5)d, & j_{T_{R/L}}^{\mu\nu} &\equiv \bar{e}\gamma^{\mu\nu}(1 \pm \gamma_5)\nu, \end{aligned} \quad (2.2)$$

where  $\gamma^{\mu\nu}$  is defined as  $\gamma^{\mu\nu} = \frac{i}{2}[\gamma^{\mu}, \gamma^{\nu}]$ . The first term of eq. (2.1) is the SM charged current interaction, the other terms contain all new physics contributions. We normalize the coefficients  $\epsilon_{\alpha}^{\beta}$  relative to the SM charged current strength  $G_F/\sqrt{2}$ . Recall,  $P_{L/R} = \frac{1}{2}(1 \mp \gamma_5)$  and we will use the subscripts  $L$  and  $R$  for left-handed and right-handed fermions, respectively. Note also that all leptonic currents with  $(1 - \gamma_5)$  will pick  $m_{\nu_i}$  from the propagator, leading to an amplitude proportional to  $\epsilon_{\alpha}^{\beta L} \times \langle m_{\nu} \rangle$  ( $\beta_L \in \{S-P, V-A, T_L\}$ ), which is always smaller than the standard mass mechanism contribution and thus is not very interesting. Thus, only six particular  $\epsilon_{\alpha}^{\beta}$  can be constrained from  $0\nu\beta\beta$  decay. For convenience, we repeat the currently best limits, all derived in [1], in table 1.

Recently, several papers have discussed QCD corrections to the decay rate for the short-range part [43, 44] and the pion-exchange (medium range) part [45] of the double beta decay amplitude. In these papers it was pointed out, that operator mixing can lead to significant changes in the limits obtained from  $0\nu\beta\beta$  decay for some specific operators. No calculation for the QCD corrections for the long-range part of the amplitude exists up to now. Thus, the limits in table 1 do not take into account the effect of these higher order corrections.

Eq. (2.1) describes long-range  $0\nu\beta\beta$  decay from the low-energy point of view. From the particle physics point of view, these  $\Delta L = 2$  currents can be described as being generated from  $d = 7$  operators. Disregarding the  $d = 7$  ‘‘Weinberg-like’’ operator  $\mathcal{O}_W \times (H^{\dagger}H)$ , there are four of these operators in the list of Babu & Leung [15]:

$$\begin{aligned} \mathcal{O}_2 &\propto L^i L^j L^k e^c H^l \epsilon_{ij} \epsilon_{kl}, \\ \mathcal{O}_3 &\equiv \{\mathcal{O}_{3a}, \mathcal{O}_{3b}\} \propto \{L^i L^j Q^k d^c H^l \epsilon_{ij} \epsilon_{kl}, L^i L^j Q^k d^c H^l \epsilon_{ik} \epsilon_{jl}\}, \\ \mathcal{O}_4 &\equiv \{\mathcal{O}_{4a}, \mathcal{O}_{4b}\} \propto \{L^i L^j \bar{Q}_i \bar{u}^c H^k \epsilon_{jk}, L^i L^j \bar{Q}_k \bar{u}^c H^k \epsilon_{ij}\}, \\ \mathcal{O}_8 &\propto L^i \bar{e}^c \bar{u}^c d^c H^j \epsilon_{ij}. \end{aligned} \quad (2.3)$$

Here,  $\mathcal{O}_2$  is included for completeness, although it is trivial that the mass mechanism will be the dominant contribution to  $0\nu\beta\beta$  decay for this operator, since it does not involve any quark fields. We will therefore not discuss the detailed decomposition of  $\mathcal{O}_2$ , which can be found in [40]. The operators  $\mathcal{O}_{3b,4a,8}$  will contribute to the long-range amplitudes  $j_\beta J_\alpha$ , and the coefficient of the amplitudes is described as

$$\frac{G_F \epsilon_{d=7}}{\sqrt{2}} \simeq \frac{g_{\text{eff}}^3 v}{4\Lambda_7^3}, \quad (2.4)$$

where  $\Lambda_7$  is the energy scale from which the  $d = 7$  operators originate, and  $\epsilon_{d=7}$  is one of (or a combination of two of) the  $\epsilon_\alpha^\beta$  of table 1. The factor  $1/4$  is included to account for the fact that eq. (2.2) is written in terms of  $(1 \pm \gamma_5)$  while chiral fields are defined using  $P_{L/R}$ . This leads to the numerical constraints on the scale  $\Lambda_7$  mentioned in the introduction, taking the least/most stringent numbers from table 1.

All  $\Delta L = 2$  operators generate Majorana neutrino masses. However, operators  $\mathcal{O}_{3a}$  and  $\mathcal{O}_{4b}$  will generate neutrino mass matrices without diagonal entries, since  $L^i L^j \epsilon_{ij} = 0$  within a generation. Neutrino mass matrices with such a flavour structure result in very restricted neutrino spectra, and it was shown in [47] that such models necessarily predict  $\sin^2(2\theta_{12}) = 1 - (1/16)(\Delta m_{21}^2/\Delta m_{31}^2)^2$ . This prediction is ruled out by current neutrino data at more than  $8 \sigma$  c.l. [5]. Models that generate at low energies only  $\mathcal{O}_{3a}$  or  $\mathcal{O}_{4b}$  can therefore not be considered realistic explanation of neutrino data.<sup>5</sup>

Flavour off-diagonality of  $\mathcal{O}_{3a}$  and  $\mathcal{O}_{4b}$  does also suppress strongly their contribution to long-range double beta decay, in case the resulting leptonic current is of type  $j_{S+P}$  (see appendix<sup>6</sup>). This is because the final state leptons are both electrons, while the virtual neutrino emitted from the  $L$  in  $\mathcal{O}_{3a,4b}$  is necessarily either  $\nu_\mu$  or  $\nu_\tau$ . In the definition of the “effective”  $\epsilon_\alpha^\beta$ , then neutrino mixing matrices appear with the combination  $\sum_j U_{ej} U_{\mu j}^*$  (or  $U_{ej} U_{\tau j}^*$ ), which is identically zero unless the mixing matrices are non-unitary when summed over the light neutrinos.

Departures from unitarity can occur in models with extra (sterile/right-handed) neutrinos heavier than about  $\sim 1$  GeV. While the propagation of the heavy neutrinos also contributes to  $0\nu\beta\beta$ , the nuclear matrix element appearing in the amplitude of the heavy neutrino exchange is strongly suppressed, when their masses are larger than 1 GeV [49, 50]. Consequently, the heavy neutrino contribution is suppressed with respect to the light neutrino one and the sum over  $\sum_j U_{ej} U_{\mu j}^*$  is incomplete, appearing effectively as a sum over mixing matrix elements which is non-unitary. Current limits on this non-unitary piece of the mixing are of the order of very roughly percent [51–54], thus weakening limits on the coefficients for  $\mathcal{O}_{3a}$  and  $\mathcal{O}_{4b}$  (for  $j_{S+P}$ ), compared to other operators, by *at least* two orders of magnitude.

---

<sup>5</sup>However, models that produce these operators usually allow to add additional interactions that will generate  $\mathcal{O}_5$  ( $\mathcal{O}_6$ ) in addition to  $\mathcal{O}_{3a}$  ( $\mathcal{O}_{4b}$ ), as for example in the model discussed in [48]. These constructions then allow to correctly explain neutrino oscillation data, since  $\mathcal{O}_5/\mathcal{O}_6$  produce non-zero elements in the diagonal entries of the neutrino mass matrix.

<sup>6</sup>Decomposition #8 of  $\mathcal{O}_{3a}$  also generates  $j_{T_R}$  which can contribute to  $0\nu\beta\beta$  without the need for a non-unitarity of the mixing matrix.

To the list in eq. (2.3) one can add two more  $\Delta L = 2$  operators involving derivatives:

$$\begin{aligned} \mathcal{O}_1^{D\mu} &\equiv \{\mathcal{O}_{1a}^{D\mu}, \mathcal{O}_{1b}^{D\mu}\} \propto \{L^i L^j D_\mu D_\mu H^k H^l \epsilon_{ij\epsilon_{kl}}, L^i L^j D_\mu D_\mu H^k H^l \epsilon_{ik\epsilon_{jl}}\} \\ \mathcal{O}_2^{D\mu} &\propto L^i e^c D_\mu H^j H^k H^l \epsilon_{ij\epsilon_{kl}} \end{aligned} \quad (2.5)$$

We mention these operators for completeness. As shown in [55], tree-level decompositions of  $\mathcal{O}_1^{D\mu}$  always involve one of the seesaw mediators, and thus one expects this operator to be always present in tree-level models of neutrino mass. As we will see, if neutrino masses are generated from tree-level, the mass mechanism contribution in general dominates  $0\nu\beta\beta$ , and consequently the new physics effect from  $\mathcal{O}_1^{D\mu}$  cannot make a measurable impact. The second type of the derivative operators,  $\mathcal{O}_2^{D\mu}$ , has also been discussed in detail in [55] with an example of tree-level realization, we thus give only a brief summary for this operator in the appendix.

### 3 Classification

In this section we will discuss a classification scheme for the decompositions of the  $\Delta L = 2$  operators of eq. (2.3), based on the number of loops, at which they generate neutrino masses. We will discuss one typical example each for tree-level, 1-loop and 2-loop models. The complete list of decompositions for the different cases can be found in the appendix.

#### 3.1 Tree level

If the neutrino mass is generated at tree-level, one expects  $m_\nu \propto v^2/\Lambda$ , which for coefficients of  $\mathcal{O}(1)$  give  $\Lambda \sim 10^{14}$  GeV for neutrino masses order 0.1 eV. The amplitude of the mass mechanism of  $0\nu\beta\beta$  decay is proportional to  $\mathcal{A}^{\text{MM}} \propto \langle m_\nu \rangle / p_F^2 \times (1/m_W^2)^2$ , while the amplitude provided from the  $d = 7$  operator is  $\mathcal{A}^{\text{LR}} \propto p_F v / (\Lambda^3 p_F^2) \times (1/m_W^2)$ . The  $d = 7$  contribution is therefore favoured by a factor  $p_F / \langle m_\nu \rangle$ , but suppressed by  $(v/\Lambda)^3$ . Inserting  $\Lambda \sim 10^{14}$ , the  $d = 7$  amplitude should be smaller than the mass mechanism amplitude by a huge factor of order  $\mathcal{O}(10^{-27})$ . However, this naive estimate assumes all coefficients in the operators to be order  $\mathcal{O}(1)$ . Since these coefficients are usually products of Yukawa (and other) couplings in the UV complete models, this is not necessarily the case in general and much smaller scales  $\Lambda$  could occur.

To discuss this in a bit more detail, we consider a particular example based on  $\mathcal{O}_3$ , decomposition #4, where two new fields, (1) a Majorana fermion  $\psi$  with the SM charge  $(\text{SU}(3)_c, \text{SU}(2)_L, \text{U}(1)_Y) = (1, 1, 0)$  and (2) a scalar  $S$  with  $(3, 2, 1/6)$ , are introduced to decompose the effective operator, see table 3 and figure 1. The Lagrangian for this model contains the following terms:

$$\mathcal{L}_{3,\#4} = Y_\nu \bar{\psi} H \cdot L + Y_{d^c L} \bar{d}_R L \cdot S + Y_{Q\psi} \bar{\psi} Q \cdot S^\dagger + m_\psi \bar{\psi}^c \psi + \text{h.c.} \quad (3.1)$$

Here, we have suppressed generation indices for simplicity. The first term in eq. (3.1) will generate Dirac masses for the neutrinos. The Majorana mass term for the neutral field  $\psi$  (equivalent to a right-handed neutrino) can not be forbidden in this model. We will discuss



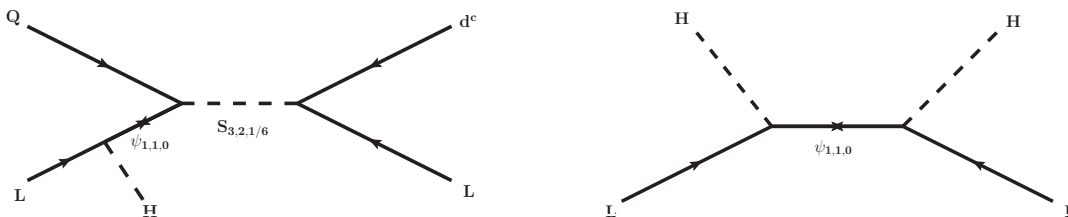


**Figure 1.** To the left: diagram leading to long-range  $0\nu\beta\beta$  decay via charged scalar exchange for Babu-Leung operator  $\mathcal{O}_3$  (BL#3). To the right: tree-level neutrino mass generated via seesaw type-I, using the same vertices as in the diagram on the left. Here and in all Feynman diagrams below, arrows on fermion lines indicate the flow of particle number, not the chirality of the fermion. The double arrow on  $\psi_{1,1,0}$  indicates its Majorana nature.

first the simplest case with only one copy of  $\psi$  and comment on the more complicated cases with two or three  $\psi$  below.

The contribution to  $0\nu\beta\beta$  decay can be read off directly from the diagram in figure 1 on the left. It is given by

$$\frac{GF\epsilon_{\mathcal{O}_{3,\#4}}}{\sqrt{2}} \simeq \frac{(Y_\nu)_e v}{m_\psi} \frac{(Y_{d^c L})_{1e} (Y_{Q\psi})_1}{m_S^2}. \quad (3.2)$$

With only one copy of  $\psi$ , the effective mass term contributing to  $0\nu\beta\beta$  decay is  $\langle m_\nu \rangle = (Y_\nu)_e^2 v^2 / m_\psi$  and we can replace  $(Y_\nu)_e$  by  $\langle m_\nu \rangle$  to arrive at the rough estimate of the constraint derived from the  $d = 7$  contribution to  $0\nu\beta\beta$ :

$$(Y_{d^c L})_{1e} (Y_{Q\psi})_1 \lesssim 3 \times 10^{-3} \left( \frac{\langle m_\nu \rangle}{0.5 \text{ eV}} \right)^{-1/2} \left( \frac{m_\psi}{100 \text{ GeV}} \right)^{1/2} \left( \frac{m_S}{1 \text{ TeV}} \right)^2 \quad (3.3)$$

Eq. (3.3) shows that the upper limit on the Yukawa couplings disappears as  $\langle m_\nu \rangle$  approaches zero. When the masses are greater than roughly  $m_\psi \simeq m_S \sim 10 \text{ TeV}$ , the Yukawa couplings must be non-perturbative to fulfil the equality in eq. (3.3). This implies that the mass mechanism will always dominate the  $0\nu\beta\beta$  contribution for scales  $\Lambda$  larger than roughly this value, independent of the exact choice of the couplings.

We briefly comment on models with more than one  $\psi$ . As is well-known, neutrino oscillation data require at least two non-zero neutrino masses, while a model with only one  $\psi$  leaves two of the three active neutrinos massless. Any realistic model based on eq. (3.1) will therefore need at least two copies of  $\psi$ . In this case eq. (3.2) has to be modified to include the summation over the different  $\psi_i$  and  $\epsilon_{\mathcal{O}_{3,\#4}} \propto \sum_i \frac{(Y_\nu)_{ei} v}{m_{\psi_i}}$ .  $\langle m_\nu \rangle$ , on the other hand, is proportional to  $\langle m_\nu \rangle \propto \sum_i \frac{(Y_\nu)_{ei}^2}{m_{\psi_i}}$ . In this case, one still expects in general that limits derived from the long-range part of the amplitude are proportional to  $\langle m_\nu \rangle$ . However, there is a special region in parameter space, where the different contributions to  $\langle m_\nu \rangle$  cancel nearly exactly, leaving the long-range contribution being the dominant part of the amplitude. Unless the model parameters are fine-tuned in this way, the mass mechanism should win over the  $d = 7$  contribution for all tree-level neutrino mass models.

The tables in the appendix show, that all three types of seesaw mediators appear in the decompositions of  $\mathcal{O}_3$ ,  $\mathcal{O}_4$  and  $\mathcal{O}_8$ :  $\psi_{1,1,0}$  (type-I),  $\psi_{1,3,0}$  (type-III) and  $S_{1,3,1}$  (type-II).



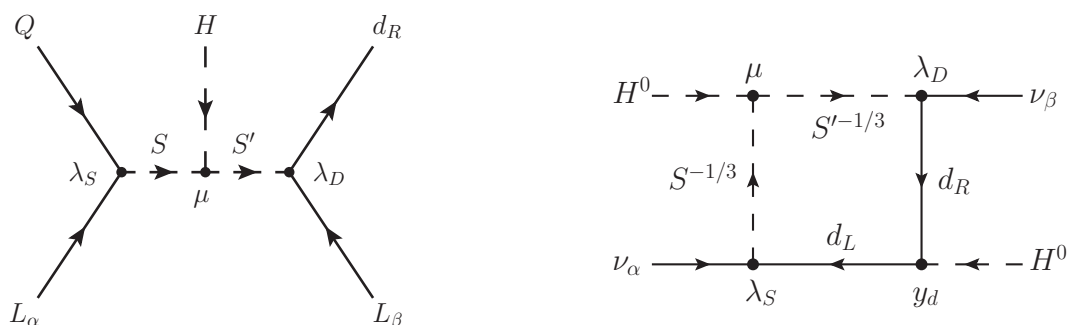


**Figure 2.** Decomposition #2 of  $\mathcal{O}_3$  operator (left) and one-loop diagram for neutrino masses based on the decomposition (right).

In order to generate a seesaw mechanism, for some of the decompositions one needs to introduce new interactions, such as  $S_{1,3,1}^\dagger HH$ , not present in the corresponding decomposition itself. However, in all these cases, the additional interactions are allowed by the symmetries of the models and are thus expected to be present. One then expects for all tree-level decompositions that the mass mechanism dominates over the long-range part of the amplitude, unless (i) the new physics scale  $\Lambda$  is below a few TeV *and* (ii) some parameters are extremely fine-tuned to suppress light neutrino masses, as discussed above in our particular example decomposition.

### 3.2 One-loop level

We now turn to a discussion of one-loop neutrino mass models. For this class of neutrino mass models, naive estimates would put  $\Lambda$  at  $\Lambda \sim \mathcal{O}(10^{12})$  GeV for coefficients of  $\mathcal{O}(1)$  and neutrino masses of  $\mathcal{O}(0.1)$  eV. Thus, in the same way as tree neutrino mass models, the mass mechanism dominates over the long-range amplitude, unless at least some of the couplings in the UV completion are significantly smaller than  $\mathcal{O}(1)$ , as discussed next.

As shown in [56], there are only three genuine 1-loop topologies for ( $d = 5$ ) neutrino masses. Decompositions of  $\mathcal{O}_3$ ,  $\mathcal{O}_4$  or  $\mathcal{O}_8$  produce only two of them, namely  $T\nu$ -I-ii or  $T\nu$ -I-iii. We will discuss one example for  $T\nu$ -I-ii, based on  $\mathcal{O}_3$  decomposition #2, see table 3 and figure 2. The underlying leptoquark model was first discussed in [36, 57], and for accelerator phenomenology see, e.g., [58]. The model adds two scalar states to the SM particle content,  $S(3, 1, -1/3)$  and  $S'(3, 2, 1/6)$ . The Lagrangian of the model contains interactions with SM fermions

$$\mathcal{L}_{3,\#2}^{\text{LQ}} = (\lambda_S)_{\alpha i} \overline{L}_\alpha^c \cdot Q_i S^\dagger + (\lambda_D)_{i\alpha} \overline{d}_{Ri} L_\alpha \cdot S' + \dots, \quad (3.4)$$

and the scalar interactions and mass terms:

$$\mathcal{L}_{3,\#2}^{\text{scalar}} = \mu SH \cdot S'^\dagger + m_S^2 |S|^2 + m_D^2 |S'|^2 + \dots \quad (3.5)$$

Lepton number is violated by the simultaneous presence of the terms in eq. (3.4) and the first term in eq. (3.5) [57]. Electro-weak symmetry breaking generates the off-diagonal

element of the mass matrix for the scalars with the electric charge  $-1/3$ . The mass matrix is expressed as

$$M_{\text{LQ}}^2 = \begin{pmatrix} m_S^2 & \mu v \\ \mu v & m_D^2 \end{pmatrix} \quad (3.6)$$

in the basis of  $(S^{-1/3}, S'^{-1/3})$ , which is diagonalized by the rotation matrix with the mixing angle  $\theta_{\text{LQ}}$  that is given as

$$\tan 2\theta_{\text{LQ}} = \frac{2\mu v}{m_S^2 - m_D^2}. \quad (3.7)$$

The neutrino mass matrix, which arises from the 1-loop diagram shown in figure 2, is calculated to be

$$(m_\nu)_{\alpha\beta} = \frac{N_c \sin 2\theta_{\text{LQ}}}{2(16\pi^2)} \sum_k m_{d_k} \Delta B_0(m_{d_k}^2, m_1^2, m_2^2) \left\{ (\lambda_S)_{\alpha k} (\lambda_D)_{k\beta} + (\alpha \leftrightarrow \beta) \right\}, \quad (3.8)$$

where  $N_c = 3$  is the colour factor. The loop-integral function  $\Delta B_0$  is given as

$$\Delta B_0(m_{d_k}^2, m_1^2, m_2^2) = \frac{m_1^2 \ln(m_1^2/m_{d_k}^2)}{m_1^2 - m_{d_k}^2} - \frac{m_2^2 \ln(m_2^2/m_{d_k}^2)}{m_2^2 - m_{d_k}^2}. \quad (3.9)$$

with the eigenvalues  $m_{1,2}^2$  of the leptoquark mass matrix eq. (3.6) and the mass  $m_{d_k}$  of the down-type quark of the  $k$ -th generation. Due to the hierarchy in the down-type quark masses, it is expected that the contribution from  $m_b$  dominates the neutrino mass eq. (3.8). For  $m_b \ll \bar{M}$  and  $\mu v \ll \bar{M}^2$  where  $\bar{M} = m_D^2 = m_S^2$ , eq. (3.8) is reduced to

$$(m_\nu)_{\alpha\beta} = \frac{3}{16\pi^2} \frac{\mu v}{\bar{M}^2} m_b \left\{ (\lambda_S)_{\alpha 3} (\lambda_D)_{3\beta} + (\alpha \leftrightarrow \beta) \right\}, \quad (3.10)$$

and this gives roughly

$$(\lambda_S)_{e3} (\lambda_D)_{3e} = 10^{-2} \left( \frac{\langle m_\nu \rangle}{0.2\text{eV}} \right) \left( \frac{1\text{MeV}}{\mu} \right) \left( \frac{\bar{M}}{1\text{TeV}} \right)^2. \quad (3.11)$$

The constraint on the effective neutrino mass  $\langle m_\nu \rangle \lesssim 0.2\text{eV}$  is derived from the combined KamLAND-Zen and EXO data [46], which is  $T_{1/2} \geq 3.4 \times 10^{25}$  ys for  $^{136}\text{Xe}$ . The same experimental results also constrain the coefficient of the  $d = 7$  operator generated from the Lagrangians eqs. (3.4) and (3.5) as  $\epsilon_{T_R}^{T_R} \lesssim 5.6 \times 10^{-10}$  (cf. table 1), which gives

$$(\lambda_S)_{e1} (\lambda_D)_{1e} \lesssim 3 \cdot 10^{-2} \left( \frac{1\text{MeV}}{\mu} \right) \left( \frac{\bar{M}}{1\text{TeV}} \right)^4 \quad (3.12)$$

Therefore, for  $(\lambda_S)_{e1} (\lambda_D)_{1e} \simeq (\lambda_S)_{e3} (\lambda_D)_{3e}$ , the mass mechanism and the  $d = 7$  contribution are approximately of equal size with  $\bar{M} \simeq 750\text{GeV}$ . Since  $\langle m_\nu \rangle \propto \bar{M}^{-2}$ , while  $\epsilon_{\mathcal{O}_{3,\#2}} \propto \bar{M}^{-4}$ , the mass mechanism will dominate  $0\nu\beta\beta$  decay for  $\bar{M}$  larger than  $\bar{M} \simeq 750\text{GeV}$ , unless the couplings  $(\lambda_S)_{e1} (\lambda_D)_{1e}$  are larger than  $(\lambda_S)_{e3} (\lambda_D)_{3e}$ . We note that, leptoquark searches by the ATLAS [59, 60] and the CMS [61–63] collaborations have provided lower limits on the masses of the scalar leptoquarks, depending on the lepton generation they couple to and also on the decay branching ratios of the leptoquarks. The

limits derived from the search for the pair-production of leptoquarks are roughly in the range 650 – 1000 GeV [59–63], depending on assumptions.

The other 1-loop models are qualitatively similar to the example discussed above. However, the numerical values for masses and couplings in the high-energy completions should be different, depending on the Lorentz structure of the  $d = 7$  operators, see also the appendix.

### 3.3 Two-loop level

We now turn to a discussion of 2-loop neutrino mass models. As shown in the appendix, in case of the operators  $\mathcal{O}_3$  and  $\mathcal{O}_4$ , 2-loop models appear only for the cases  $\mathcal{O}_{3a}$  and  $\mathcal{O}_{4b}$ . As explained in section 2, these operators alone cannot give realistic neutrino mass models. We thus base our example model on  $\mathcal{O}_8$ . The 2-loop neutrino mass models based on  $\mathcal{O}_8$  are listed in table 5 in the appendix. In this section, we will discuss decomposition #15, since it has not been discussed in detail in the literature before.

In this model, we add the following states to the SM particle content:

$$(\psi_{L,R})_{3,2,7/6} = \begin{pmatrix} \psi_{L,R}^{5/3} \\ \psi_{L,R}^{2/3} \end{pmatrix}, \quad (3.13)$$

$$(S_{3,2,1/6})_k = \begin{pmatrix} S_k^{2/3} \\ S_k^{-1/3} \end{pmatrix}. \quad (3.14)$$

With the new fields, we have the interactions

$$\mathcal{L}_{8,\#15} = Y_{d_i L_\alpha S_k} \overline{d_{R,i}} L_\alpha \cdot S_k + Y_{u_i \psi H} \overline{u_{R,i}} \psi_L H^\dagger + Y_{e_\alpha \psi S_k} \overline{e_{R\alpha}} \psi_R S_k^\dagger + \text{h.c.}, \quad (3.15)$$

which mediate  $\mathcal{O}_8$  operator, as shown in the left diagram of figure 3. Here,  $i$  runs over the three quark generations. While  $Y_{d_i L_\alpha S_k}$  and  $Y_{u_i \psi H}$  could be different for different  $i$ , for simplicity we will assume the couplings to quarks are the same for all  $i$  and drop the index  $i$  in the following. We will comment below, when we discuss the numerical results, on how this choice affects phenomenology. For simplicity, we introduce only one generation of the new fermion  $\psi$ , while we allow for more than one copy of the scalar  $S_{3,2,1/6}$ . Note that, in principle, the model would work also for one copy of  $S_{3,2,1/6}$  and more than one  $\psi$ , but as we will see later, the fit to neutrino data becomes simpler in our setup.

The fermion  $\psi^{2/3}$  mixes with the up-type quarks through the following mass term:

$$\begin{aligned} \mathcal{L}_{\text{mass}} &= Y_u \langle H^0 \rangle \overline{u_L} u_R + M_\psi \overline{\psi_L^{2/3}} \psi_R^{2/3} + Y_{u\psi H}^\dagger \langle H^0 \rangle \overline{\psi_L^{2/3}} u_R + \text{h.c.}, \\ &= \begin{pmatrix} \overline{t_L} & \overline{\psi_L^{2/3}} \end{pmatrix} \begin{pmatrix} m_t & 0 \\ \Delta & M_\psi \end{pmatrix} \begin{pmatrix} t_R \\ \psi_R^{2/3} \end{pmatrix} + \text{h.c.}, \end{aligned} \quad (3.16)$$

where  $\Delta \equiv Y_{u\psi H}^\dagger \langle H^0 \rangle$ . Due to the strong hierarchy in up-type quark masses, we have assumed the sub-matrix for the up-type quarks in eq. (3.16) is completely dominated by the contribution from top quarks. The mass matrix eq. (3.16) is diagonalized with the

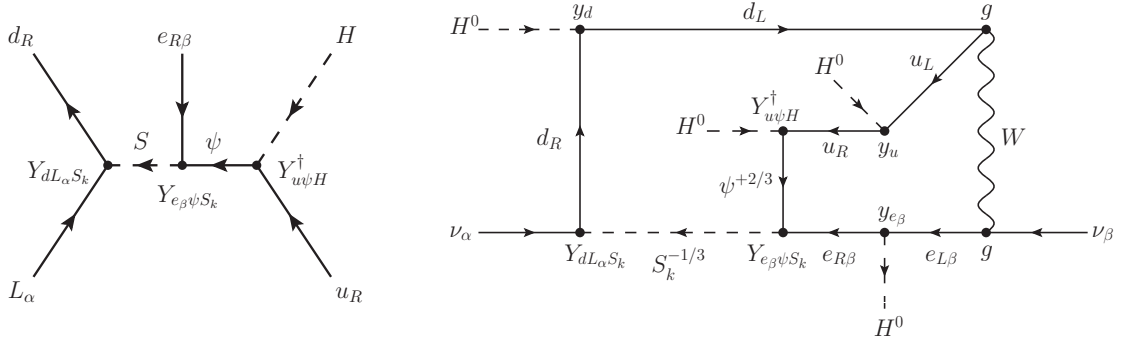


**Figure 3.** Decomposition #15 of  $\mathcal{O}_8$  operator (left) and two-loop diagram for neutrino masses based on the decomposition (right).

unitary matrices  $V_L$  and  $V_R$  as

$$V_L^\dagger \begin{pmatrix} m_t & 0 \\ \Delta & M_\psi \end{pmatrix} V_R = \text{diag}(M_{\Psi_i}), \quad (3.17)$$

and the mass eigenstates  $\Psi_i^{2/3}$  are give as

$$\begin{pmatrix} t_L \\ \psi_L^{2/3} \end{pmatrix}_a = (V_L)_{ai} \Psi_{Li}^{2/3} \quad \text{and} \quad \begin{pmatrix} t_R \\ \psi_R^{2/3} \end{pmatrix}_a = (V_R)_{ai} \Psi_{Ri}^{2/3}, \quad (3.18)$$

where the index  $a$  for the interaction basis takes  $a \in \{t, \psi\}$ . The interactions are written in the mass eigenbasis as follows:

$$\mathcal{L}_W = \frac{g}{\sqrt{2}} (V_L^\dagger)_{it} \overline{\Psi_i^{2/3}} \gamma^\rho P_L b W_\rho^+ + \text{h.c.}, \quad (3.19)$$

$$\mathcal{L}_S = Y_{dL_\alpha S_k} \overline{d_R} L_\alpha \epsilon S_k + Y_{e_\alpha \psi S_k} (V_R)_{\psi i} \overline{e_\alpha^c} P_R \Psi_i^{2/3} S_k^{-1/3\dagger} + Y_{e_\alpha \psi S_k} \overline{e_\alpha^c} P_R \psi^{5/3} S_k^{2/3\dagger} + \text{h.c.} \quad (3.20)$$

The 2-loop neutrino mass diagram generated by this model is shown in figure 3. Using the formulas given in [64], one can express the neutrino mass matrix as

$$(m_\nu)_{\alpha\beta} = \frac{N_c g^2 m_b (V_L^\dagger)_{it} (V_R)_{\psi i}}{2(16\pi^2)^2 M_{\Psi_i}} [m_{e_\alpha} Y_{dL_\beta S_k} Y_{e_\alpha \psi S_k} + m_{e_\beta} Y_{dL_\alpha S_k} Y_{e_\beta \psi S_k}] I(z_{k,i}, r_i, t_i). \quad (3.21)$$

Here  $N_c = 3$  is the colour factor and  $I(z_{k,i}, r_i, t_i)$  is the loop integral defined as

$$I(z_{k,i}, r_i, t_i) = \left[ 4\hat{I}(z_{k,i}, r_i, t_i) - \frac{1}{t_i} \hat{I}^{(k^2)}(z_{k,i}, r_i, t_i) \right], \quad (3.22)$$

with

$$\hat{I}(z_{k,i}, r_i, t_i) = \frac{1}{\pi^4} \int d^4 q \int d^4 k \frac{1}{(q^2 - z_{k,i})(q^2 - r_i)(k^2 - t_i)k^2((q+k)^2 - 1)}, \quad (3.23)$$

$$\hat{I}^{(k^2)}(z_{k,i}, r_i, t_i) = \frac{1}{\pi^4} \int d^4 q \int d^4 k \frac{k^2}{(q^2 - z_{k,i})(q^2 - r_i)(k^2 - t_i)k^2((q+k)^2 - 1)}, \quad (3.24)$$

The dimensionless parameters  $z_{k,i}, r_i, t_i$  are defined as

$$z_{k,i} \equiv \frac{m_{S_k}^2}{M_{\Psi_i}^2}, \quad r_i \equiv \frac{m_b^2}{M_{\Psi_i}^2}, \quad \text{and} \quad t_i \equiv \frac{M_W^2}{M_{\Psi_i}^2} \quad (3.25)$$

and loop momenta  $q$  and  $k$  are also defined dimensionless. Due to the strong hierarchy in down-type quark masses, we expect that neutrino mass given in eq. (3.21) is dominated by the contribution from bottom quark. If we assume in eq. (3.21) that all Yukawa couplings are of the same order, then the entries of the neutrino mass matrix will have a strong hierarchy:  $(m_\nu)_{ee} : (m_\nu)_{\mu\mu} : (m_\nu)_{\tau\tau} = m_e : m_\mu : m_\tau$ . Such a flavor structure is not consistent with neutrino oscillation data. Therefore, in order to reproduce the observed neutrino masses and mixings, our Yukawa couplings need to have a certain compensative hierarchy in their flavor structure.

Since the neutrino mass matrix, and thus the Yukawa couplings contained in the neutrino mass, have a non-trivial flavour pattern, these Yukawas will be also constrained by charged lepton flavour violation (LFV) searches. Here we discuss only  $\mu \rightarrow e\gamma$  which usually provides the most stringent constraints in many models. In order to calculate the process  $\mu \rightarrow e\gamma$  we adapt the general formulas shown in [65] for our particular case. The amplitude for  $\mu \rightarrow e\gamma$  decay is given by

$$\mathcal{M}(\mu \rightarrow e\gamma) = e\epsilon_\alpha^* q_\beta \bar{u}(p_e) i\sigma^{\alpha\beta} (\sigma_R P_R + \sigma_L P_L) u(p_\mu). \quad (3.26)$$

Here,  $\epsilon_\alpha$  is the photon polarization vector and  $q_\beta$  is the momentum of photon. Three different diagrams contribute to the amplitude for  $\mu \rightarrow e\gamma$ , which are finally summarized with the two coefficients  $\sigma_R$  and  $\sigma_L$  given by

$$\sigma_R = i \frac{m_\mu}{16\pi^2} \left[ Y_{dL_2 S_k}^\dagger Y_{dL_1 S_k} \frac{2F_2(x_{b,k}) - F_1(x_{b,k})}{m_{S_k}^2} \right], \quad (3.27)$$

$$\sigma_L = i \frac{m_\mu}{16\pi^2} \left[ Y_{e_2 \psi S_k}^\dagger Y_{e_1 \psi S_k} \frac{-F_2(x_{\psi,k}) - 7F_1(x_{\psi,k})}{m_{S_k}^2} \right], \quad (3.28)$$

where  $x_{\psi,k} \equiv \frac{M_\psi^2}{m_{S_k}^2}$  and  $x_{b,k} \equiv \frac{m_b^2}{m_{S_k}^2}$ . Here, we have assumed that both the  $\psi^{-2/3}$  and the  $\psi^{-5/3}$  have the same mass  $M_\psi$ . This neglects (small) mass shifts in the  $\psi^{-2/3}$  state, due to its mixing with the top quark. Due to the large value of  $M_\psi$ , that we use in our numerical examples, this should be a good approximation. Note also, that the contribution from the top quark is negligible for those large values of  $M_\psi$  used below. The functions  $F_1(x)$  and  $F_2(x)$  are defined in eqs. (40) and (41) in [65] as

$$F_1(x) = \frac{x^2 - 5x - 2}{12(x-1)^3} + \frac{x \ln x}{2(x-1)^4}, \quad (3.29)$$

$$F_2(x) = \frac{2x^2 + 5x - 1}{12(x-1)^3} - \frac{x^2 \ln x}{2(x-1)^4}, \quad (3.30)$$

The branching ratio for  $\mu \rightarrow e\gamma$  can be expressed with the coefficients  $\sigma_R$  and  $\sigma_L$  as

$$\text{Br}(\mu \rightarrow e\gamma) = \frac{e^2 m_\mu^3 (|\sigma_R|^2 + |\sigma_L|^2)}{16\pi \Gamma_\mu}, \quad (3.31)$$

where  $\Gamma_\mu$  is the total decay width of muon. Later, we will numerically calculate the branching ratio to search for the parameter choices that are consistent with the oscillation data and the constraint from  $\mu \rightarrow e\gamma$ .

Before discussing constraints from lepton flavour violation, we will compare the long-range contribution to  $0\nu\beta\beta$  with the mass mechanism in this model. This model manifestly generates a  $d = 7$  long-range contribution to  $0\nu\beta\beta$ . The half-life of  $0\nu\beta\beta$  induced by the long-range contribution is proportional to the coefficient  $\epsilon_{V+A}^{V+A}$  which is expressed in terms of the model parameters as

$$\epsilon_{V+A}^{V+A} = \frac{\sqrt{2}}{G_F} \frac{\Delta}{M_\psi} \frac{Y_{e_1\psi S_k} Y_{dL_1 S_k}}{2m_{S_k}^2} \lesssim 3.9 \times 10^{-7}. \quad (3.32)$$

Here, we use the limit on  $\epsilon_{V+A}^{V+A}$  from non-observation of  $^{136}\text{Xe}$   $0\nu\beta\beta$  decay, see table 1. With one copy of the new scalar, the bound of eq. (3.32) is directly related to the effective neutrino mass eq. (3.21) and places the stringent constraint:

$$\langle m_\nu \rangle \lesssim 2 \times 10^{-5} [\text{eV}] \left( \frac{m_S}{10[\text{TeV}]} \right)^2 \left( \frac{I(z_{k,1}, r_1, t_1)}{5 \times 10^{-2}} \right), \quad (3.33)$$

where we have used the approximate relation

$$\frac{(V_L^\dagger)_{it} (V_R)_{\psi i} I(z_{k,i}, r_i, t_i)}{M_{\Psi_i}} \simeq \frac{I(z_{k,1}, r_1, t_1) \Delta}{M_\psi m_t}, \quad (3.34)$$

with  $z_{k,1} = (m_{S_k}/m_t)^2$ ,  $r_1 = (m_b/m_t)^2$ ,  $t_1 = (M_W/m_t)^2$ , and  $I(z_{k,1}, r_1, t_1) \sim 5 \times 10^{-2}$  for a scalar mass of  $m_S = 10 \text{ TeV}$  and  $M_\psi \simeq 0.8 \text{ TeV}$ . Note that this parameter choice is motivated by the fact that the model cannot fit neutrino data with perturbative Yukawa couplings with scalar masses larger than  $m_S \gtrsim 10 \text{ TeV}$ . As one can see from eq. (3.33), the long-range contribution to  $0\nu\beta\beta$  clearly dominates over the mass mechanism in this setup.

In short, this neutrino mass model predicts large decay rate of  $0\nu\beta\beta$  but tiny  $\langle m_\nu \rangle$ . This implies that, if future neutrino oscillation experiments determine that the neutrino mass pattern has normal hierarchy but  $0\nu\beta\beta$  is discovered in the next round of experiments, the  $0\nu\beta\beta$  decay rate is dominated by the long-range part of the amplitude. Recall that  $\mathcal{O}_8$  contains  $\bar{e}^c$ . This implies that the model predicts a different angular distribution than the mass mechanism, which in principle could be tested in an experiment such as Super-NEMO [66].

Note that, to satisfy the condition eq. (3.33), cancellations among different contributions to  $\langle m_\nu \rangle$  are necessary. This can be arranged only if we consider at least two generations of the new particles in the model (either the scalar  $S$  or the fermion  $\psi$ ).

Here we discuss more on the consistency of our model with the neutrino masses and mixings observed at the oscillation experiments. Instead of scanning whole the parameter space, we illustrate the parameter choice that reproduces the neutrino properties and is simultaneously consistent with the bound from lepton flavour violation. To simplify the discussion we use the following ansatz in the flavour structure of the Yukawa couplings:

$$Y_{dL_\alpha S_k} = \frac{Y_{e_\alpha \psi S_k} m_{e_\alpha}}{y} \frac{m_{e_\alpha}}{m_\mu} \quad (3.35)$$

with a dimensionless parameter  $y$ . With eq. (3.35), the neutrino mass matrix eq. (3.21) is reduced to

$$(m_\nu)_{\alpha\beta} = (\Lambda)_{\alpha k} \mathcal{I}_k (\Lambda^T)_{k\beta}, \quad (3.36)$$

where  $\Lambda$  is defined as

$$\Lambda_{\alpha k} \equiv Y_{dL_\alpha S_k} = \frac{Y_{e_\alpha \psi S_k} m_{e_\alpha}}{y m_\mu}, \quad (3.37)$$

and  $\mathcal{I}$  is given as

$$\mathcal{I}_k = \frac{N_c g^2 y m_b m_\mu (V_L^\dagger)_{it} (V_R)_{\psi i}}{(16\pi^2)^2 M_{\Psi_i}} I(z_{k,i}, r_i, t_i). \quad (3.38)$$

We introduce three copies of the new scalar  $S_k^{-1/3}$ . The resulting mass matrix eq. (3.36) has the same index structure as that of the type-I seesaw mechanism, and therefore, the matrix  $\Lambda$  can be expressed as

$$(\Lambda^T)_{k\alpha} = \left(\sqrt{\mathcal{I}^{-1}}\right)_k R_{ki} \left(\sqrt{\hat{m}_\nu}\right)_i \left(U_\nu^\dagger\right)_{i\alpha}, \quad (3.39)$$

following the parameterization developed by Casas and Ibarra [67].

Here,  $\hat{m}_\nu$  is the neutrino mass matrix in the mass eigenbasis, and the mass matrix  $m_\nu$  is diagonalized with the lepton mixing matrix  $U_\nu$  as

$$(\hat{m}_\nu)_i \equiv \text{diag} \left( m_{\nu_1} \ m_{\nu_2} \ m_{\nu_3} \right) = (U_\nu^T)_{i\alpha} (m_\nu)_{\alpha\beta} (U_\nu)_{\beta j} \quad (3.40)$$

for which we use the following standard parametrization

$$U_\nu = \begin{pmatrix} c_{12}c_{13} & s_{12}c_{13} & s_{13}e^{i\delta} \\ -s_{12}c_{23} - c_{12}s_{23}s_{13}e^{-i\delta} & c_{12}c_{23} - s_{12}s_{23}s_{13}e^{-i\delta} & s_{23}c_{13} \\ s_{12}s_{23} - c_{12}c_{23}s_{13}e^{-i\delta} & -c_{12}s_{23} - s_{12}c_{23}s_{13}e^{-i\delta} & c_{23}c_{13} \end{pmatrix} \begin{pmatrix} 1 & 0 & 0 \\ 0 & e^{i\alpha_{21}} & 0 \\ 0 & 0 & e^{i\alpha_{31}} \end{pmatrix}. \quad (3.41)$$

Here  $c_{ij} = \cos \theta_{ij}$ ,  $s_{ij} = \sin \theta_{ij}$  with the mixing angles  $\theta_{ij}$ ,  $\delta$  is the Dirac phase and  $\alpha_{21}$ ,  $\alpha_{31}$  are Majorana phases. The matrix  $R$  is a complex orthogonal matrix which can be parametrized in terms of three complex angles as

$$R = \begin{pmatrix} c_2c_3 & -c_1s_3 - s_1s_2c_3 & s_1s_3 - c_1s_2c_3 \\ c_2s_3 & c_1c_3 - s_1s_2s_3 & -s_1c_3 - c_1s_2s_3 \\ s_2 & s_1c_2 & c_1c_2 \end{pmatrix}. \quad (3.42)$$

Note that it is assumed in this procedure that the charged lepton mass matrix is diagonal. After fitting the neutrino oscillation data with the parametrization shown above, there remain  $y$ ,  $Y_{u\psi H}$  and the masses  $M_\psi$ ,  $m_{S_k}$  for  $k = 1, 2, 3$  as free parameters. For simplicity, we assume a degenerate spectrum of the heavy scalars  $m_S = m_{S_k}$ .

In figure 4-(a), we plot the half-life  $T_{1/2}^{0\nu\beta\beta}$  as a function of  $m_{\nu_1}$  for fixed values of the coupling  $Y_{u\psi H} = 0.6$  and the masses  $M_\psi = 800$  GeV and  $m_S = 10$  TeV. The parameter  $y$  is taken to be  $10^{-3}$ , since this minimizes the decay rate of  $\mu \rightarrow e\gamma$ , as we will discuss below.



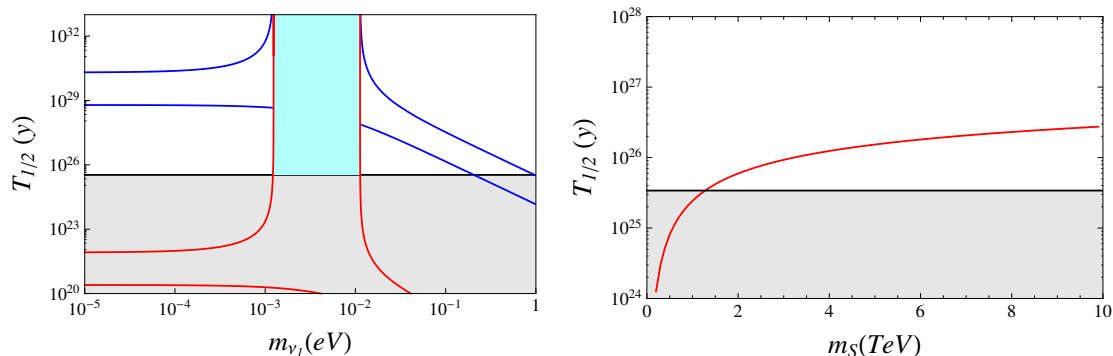


**Figure 4.** Calculated half-lives for  $0\nu\beta\beta$  decay of  $^{136}\text{Xe}$  considering the long-range contribution to the decay rate versus  $m_{\nu_1}$  (left) and  $m_S$  (right). The gray region is the current lower limit in  $0\nu\beta\beta$  decay half-life of  $^{136}\text{Xe}$ . In the plot to the left the region between the red curves is the one allowed by the long-range contribution to the decay rate of  $0\nu\beta\beta$  calculated scanning over oscillation parameters for the case of normal hierarchy and  $m_S = 10$  TeV. We also show the allowed region for the half-life for the mass mechanism as blue lines for comparison. The cyan region correspond to the parametric region where our model can be consistent with current  $0\nu\beta\beta$  experimental data. In the plot to the right the red curve is the long-range contribution to the decay rate for the fixed oscillation parameters  $m_{\nu_1} = 1.23 \times 10^{-3}$  eV,  $\alpha_{21} = 0$ ,  $\alpha_{31} = \pi/2$ ,  $s_{23}^2 = 1/2$  and  $s_{12}^2 = 1/3$  and the remaining oscillation parameters  $\Delta m_{31}^2$  and  $\Delta m_{21}^2$  fixed at their best-fit values for the case of normal hierarchy.

We have used oscillation parameters for the case of normal hierarchy. The region enclosed by the red curves is  $d = 7$  long-range contribution to  $0\nu\beta\beta$ , and the blue curves correspond to the mass mechanism contribution only, which is shown for comparison. The gray region is already excluded by  $0\nu\beta\beta$  searches, and for the model under consideration only the cyan region is allowed. As one can see from figure 4-(a), the total contribution to  $0\nu\beta\beta$  is dominated by the  $d = 7$  long-range contribution. Note that the mass mechanism and the long-range contribution are strictly related only under the assumption that  $Y_{u\psi H}$  and  $Y_{dL_\alpha S_k}$  are independent of the quark generation  $i$ . This is so, because the 2-loop diagram is dominated by 3rd generation quarks, while in  $0\nu\beta\beta$  decay only first generation quarks participate. If we were to drop this assumption and put the first generation couplings to  $Y_{u_1\psi H} \lesssim 10^{-2} \times Y_{u_3\psi H}$  and  $Y_{d_1L_\alpha S_k} \lesssim 10^{-2} \times Y_{d_3L_\alpha S_k}$ , the half-life for the long-range amplitude would become comparable to the mass mechanism, without changing the fit to oscillation data.

Note that non-zero Majorana phases are necessary to allow for cancellations among the mass mechanism contributions, so as to make  $\langle m_\nu \rangle$  small as required by eq. (3.33). In figure 4-(b), we plot the half-life  $T_{1/2}^{0\nu\beta\beta}$  as a function of the scalar mass  $m_S$ . Here we fixed the oscillation parameters to  $m_{\nu_1} = 1.23 \times 10^{-3}$  eV,  $\alpha_{21} = 0$ ,  $\alpha_{31} = \pi/2$ ,  $s_{23}^2 = 1/2$  and  $s_{12}^2 = 1/3$  and the remaining oscillation parameters  $\Delta m_{31}^2$  and  $\Delta m_{21}^2$  to their best-fit values for the case of normal hierarchy. The plot assumes that the matrix  $R$  is equal to the identity. The plot shows that the half-life increases to reach approximately  $T_{1/2}^{0\nu\beta\beta} \sim 10^{26}$  yr for  $m_S = 10$  TeV.

Now we discuss the constraint from lepton flavour violating process  $\mu \rightarrow e\gamma$ . In figure 5, we show  $\text{Br}(\mu \rightarrow e\gamma)$  as a function of the scalar  $m_S$  and the parameter  $y$  for fixed values

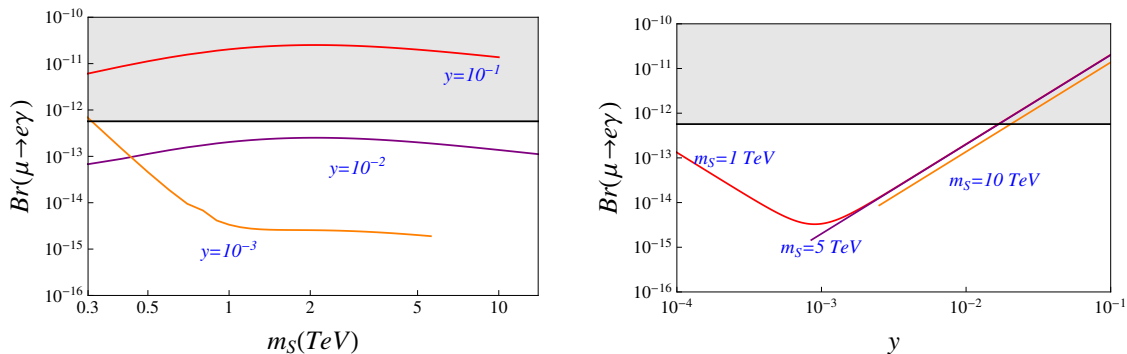


**Figure 5.**  $Br(\mu \rightarrow e\gamma)$  versus the scalar  $m_S$  (left) and the parameter  $y$  (right). In the plot to the left the red, orange and purple solid curves are the  $Br(\mu \rightarrow e\gamma)$  for different values of  $y = 10^{-1}, 10^{-2}, 10^{-3}$ . The gray region is the current experimental upper limit on  $Br(\mu \rightarrow e\gamma)$  from the MEG experiment [68]. In the plot to the right the red, orange and purple solid curves are the  $Br(\mu \rightarrow e\gamma)$  for different values of the mass  $m_S = 1, 5, 10$  TeV. We have fixed the oscillation parameters to  $m_{\nu_1} = 1.23 \times 10^{-3}$  eV,  $\alpha_{21} = 0$ ,  $\alpha_{31} = \pi/2$ ,  $s_{23}^2 = 1/2$  and  $s_{12}^2 = 1/3$ . The remaining oscillation parameters  $\Delta m_{31}^2$  and  $\Delta m_{21}^2$  are fixed at their best-fit values for the case of normal hierarchy. For discussion see text.

of the coupling  $Y_{u\psi H} = 0.6$  and the fermion mass  $M_\psi = 800$  GeV, which is the same parameter choice adopted in figure 4. These plots show that the current experimental limits on  $Br(\mu \rightarrow e\gamma)$  put strong constraints on the model under consideration. In figure 5-(a), we plot  $Br(\mu \rightarrow e\gamma)$  with different values of the parameter  $y = \{10^{-1}, 10^{-2}, 10^{-3}\}$ . We have used again the parameters  $m_{\nu_1} = 1.23 \times 10^{-3}$  eV,  $\alpha_{21} = 0$ ,  $\alpha_{31} = \pi/2$ ,  $s_{23}^2 = 1/2$  and  $s_{12}^2 = 1/3$  fixing the remaining oscillation parameters  $\Delta m_{31}^2$  and  $\Delta m_{21}^2$  at their best-fit values for the case of normal hierarchy. With the choice of  $y = 10^{-1}$ , the entire region of  $m_S$  is not consistent with the current experimental limits. On the other hand, we can easily avoid the constraint from  $\mu \rightarrow e\gamma$  by setting the parameter  $y$  to be roughly smaller than  $10^{-2}$ . Note that the curves with  $y = 10^{-1}$  and  $y = 10^{-3}$  do not cover the full range of  $m_S$ . This is because the fit to neutrino data would require Yukawa couplings in the perturbative regime. (We define the boundary to perturbativity as at least one entry in the Yukawa matrix being smaller than  $\sqrt{4\pi}$ .) It is necessary to have smaller values of the parameter  $y$  to obey the experimental bound. This feature is also shown in figure 5-(b) where we plot the  $Br(\mu \rightarrow e\gamma)$  as a function of  $y$  with different values of the mass  $m_S = \{1, 5, 10\}$  TeV. As shown, for  $y \lesssim 10^{-2}$  it is possible to fulfil the experimental limit, having the  $Br(\mu \rightarrow e\gamma)$  a minimum around  $y = 10^{-3}$ . Because of the perturbative condition, the curves with  $m_S = 5$  TeV and  $m_S = 10$  TeV end in the middle of the  $y$  space. The reason for the strong dependence of  $Br(\mu \rightarrow e\gamma)$  on the parameter  $y$  can be understood as follows: as shown in eq. (3.37) the Yukawa couplings  $Y_{dL\alpha S_k}$  and  $Y_{e\alpha\psi S_k}$  are related in the neutrino mass fit, but only up to an overall constant,  $\frac{1}{y}$ . For values of  $y$  of the order of  $10^{-3}$  both Yukawas are of the same order and this minimizes  $Br(\mu \rightarrow e\gamma)$ . If  $y$  is much larger (much smaller) than this value  $Y_{dL\alpha S_k}$  ( $Y_{e\alpha\psi S_k}$ ) becomes much larger than  $Y_{e\alpha\psi S_k}$  ( $Y_{dL\alpha S_k}$ ) and since the different diagrams contributing to  $Br(\mu \rightarrow e\gamma)$  are proportional to the individual Yukawas (and not their product) this leads to a much larger rate for  $Br(\mu \rightarrow e\gamma)$ .

In summary, for all 2-loop  $d = 7$  models of neutrino mass, which lead to  $\mathcal{O}_8$ , the long-range part of the amplitude will dominate over the mass mechanism by a large factor, unless there is a strong hierarchy between the non-SM Yukawa couplings to the first and third generation quarks. Such models are severely constrained by lepton flavour violation and  $0\nu\beta\beta$  decay. We note again, that these models predict an angular correlation among the out-going electrons which is different from the mass mechanism.

#### 4 Left-right symmetric model: $d = 7$ versus $d = 9$ operator

Writing new physics contributions to the SM in a series of NROs assumes implicitly that higher order operators are suppressed with respect to lower order ones by additional inverse powers of the new physics scale  $\Lambda$ . However, there are some particular example decompositions for (formally) higher-order operators, where this naive power counting fails. We will discuss again one particular example in more detail. The example we choose describes the situation encountered in left-right symmetric extensions of the standard model.

Consider the following two Babu-Leung operators:

$$\mathcal{O}_8 = L^i \bar{e}^c \bar{u}^c d^c H^j \epsilon_{ij} \quad \mathcal{O}_7 = L^i Q^j \bar{e}^c \bar{Q}_k H^k H^l H^m \epsilon_{il} \epsilon_{jm} \quad (4.1)$$

$\mathcal{O}_8$  can be decomposed in a variety of ways, decomposition #14 (see table 5) is shown in figure 6 to the left. The charged vector appearing in this diagram couples to a pair of right-handed quarks and, thus, can be interpreted as the charged component of the adjoint of the left-right symmetric (LR) extension of the SM, based on the gauge group  $SU(3)_C \times SU(2)_L \times SU(2)_R \times U(1)_{B-L}$ . In LR right-handed quarks are doublets,  $Q^c = \Psi_{\bar{3},1,2,-1/6}$ , the  $\psi_{1,1,0}$  can be understood as the neutral member of  $L^c$ , i.e. the right-handed neutrino, and the Higgs doublet is put into the bidoublet,  $\Phi_{1,2,2,0}$ . The resulting diagram for  $0\nu\beta\beta$  decay is shown in figure 6 on the right.

Figure 6 gives a long-range contribution to  $0\nu\beta\beta$  decay. We can estimate the size of  $\epsilon_{\mathcal{O}_8}$  from these diagrams:

$$\frac{G_F \epsilon_{\mathcal{O}_8, \#14}}{\sqrt{2}} = \frac{Y_{L\psi} g_1 g_2 v_{SM}}{m_V^2 m_\psi} = \frac{Y_{LL^c} g_R^2 v_u}{m_{W_R}^2 m_{\nu_R}} \quad (4.2)$$

The first of these two equations shows  $\epsilon_{\mathcal{O}_8}$  for figure 6 on the left (notation for SM gauge group), the second for figure 6 on the right (notation for gauge group of the LR model). Here,  $g_1$  and  $g_2$  could be different, in principle, but are equal to  $g_R$  in the LR model.  $v_{SM}$  is the SM vev, fixed by the  $W$ -mass. In the LR model, the bi-doublet(s) contain in general two vevs. We call them  $v_d$  and  $v_u$  here and  $v_{SM}^2 = v_d^2 + v_u^2$ . In eq. (4.2) only  $v_u = v_{SM} \sin \beta$ , with  $\tan \beta = v_u/v_d$ , appears. Note that we have suppressed again generation indices and summations in eq. (4.2). We will come back to this important point below.

Now, however, first consider  $\mathcal{O}_7$ . From the many different possible decompositions we concentrate on the one shown in figure 7. The diagram on the left shows the diagram in SM notation, the diagram on the right is the corresponding LR embedding. It is straightforward to estimate the size of these diagrams as:

$$\frac{G_F \epsilon_{\mathcal{O}_7}}{\sqrt{2}} = \frac{Y_{L\psi} g_1 g_2 g_3^2 v_{SM}^3}{m_{V_{1,3,0}}^2 m_{V_{1,1,1}}^2 m_\psi} = \frac{Y_{LL^c} g_L^2 g_R^2 v_u^2 v_d}{m_{W_R}^2 m_{W_L}^2 m_{\nu_R}} \propto \frac{Y_{LL^c} g_R^2 v_u}{m_{W_R}^2 m_{\nu_R}} \quad (4.3)$$

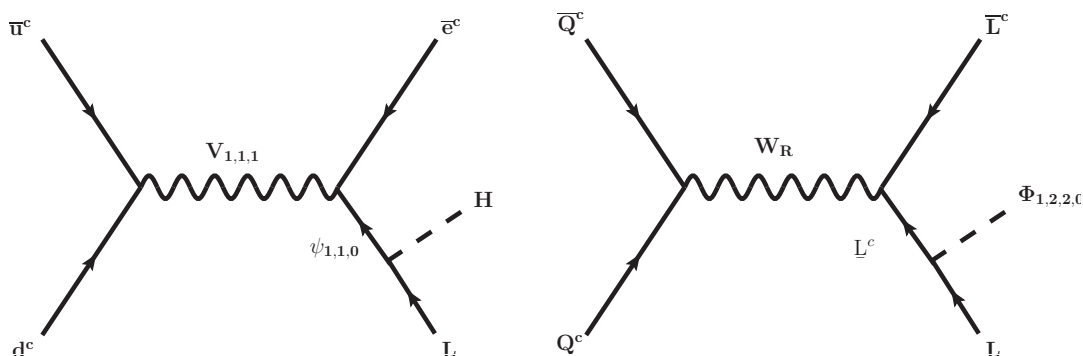


**Figure 6.**  $\mathcal{O}_8$  decomposed as #14:  $(\bar{u}^c d^c)(\bar{e}^c)(LH)$  under the SM gauge group (left) and for the LR gauge group (right).

Arbitrarily we have called the 4-point coupling in the left diagram  $g_3^2$ . In the LR model again the couplings are fixed to  $g_L$  and  $g_R$ . In the last relation in eq. (4.3) we have used  $v_{\text{SM}}^2 \propto m_{W_L}^2/g_L^2$ . This shows that eq. (4.3) is of the same order than eq. (4.2), *despite coming from a  $d = 9$  operator*. This a priori counter-intuitive result is a simple consequence of the decomposition containing the SM  $W_L$  boson. Any higher-order operator which can be decomposed in such a way will behave similarly, i.e.  $1/\Lambda^5 \Rightarrow 1/(\Lambda^3 v_{\text{SM}}^2)$ .<sup>7</sup>

We note that in this particular example the contribution of  $\mathcal{O}_7$  is actually *more stringently* constrained than the one from  $\mathcal{O}_8$ . This is because  $\mathcal{O}_8$  leads to a low-energy current of the form  $(V+A)$  in both, the leptonic *and* the hadronic indices, i.e. the limit corresponds to  $\epsilon_{V+A}^{V+A}$ .  $\mathcal{O}_7$ , on the other hand, leads to  $\epsilon_{V-A}^{V+A}$ , which is much more tightly constrained due to contribution from the nuclear recoil matrix element [69], compare values in table 1.

We note that, one can identify the diagrams in figure 6 and figure 7 with the terms proportional to  $\lambda$  and  $\eta$  in the notation of [69], used by many authors in  $0\nu\beta\beta$  decay. For recent papers on double beta decay in left-right symmetric models, see for example [70, 71]). For the complete expressions for the long-range part of the amplitude, one then has to sum over the light neutrino mass eigenstates, taking into account that the leptonic vertices in the diagrams in figures 6 and 7 are right-handed. Defining the mixing matrices for light and heavy neutrinos as  $U_{\alpha j}$  and  $V_{\alpha j}$ , respectively, as in [69], the coefficients  $\epsilon_{\mathcal{O}_8}$  and  $\epsilon_{\mathcal{O}_7}$  of the  $d = 7$  and  $d = 9$  operators are then the *effective* couplings [69]:

$$\langle \lambda \rangle = \sum_{j=1}^3 U_{ej} V_{ej} \lambda, \quad \langle \eta \rangle = \sum_{j=1}^3 U_{ej} V_{ej} \eta. \quad (4.4)$$

Orthogonality of  $U_{ej}$  and  $V_{ej}$  leads to  $\sum_{j=1}^6 U_{ej} V_{ej} \equiv 0$ . However, the sum in eq. (4.4) runs only over the light states, which does not vanish exactly, but rather is expected to be of the order of the light-heavy neutrino mixing. In left-right symmetric models with seesaw (type-I), one expects this mixing to be of order  $m_D/M_M \sim \sqrt{m_\nu/M_M}$ , where  $m_D$  is ( $M_M$ ) the Dirac mass (Majorana mass) for the (right-handed) neutrinos and  $m_\nu$

<sup>7</sup>In addition to the case of the SM W-boson, discussed here, similar arguments apply to decompositions containing the scalar  $S_{1,2,1/2}$ , which can be interpreted as the SM Higgs boson.

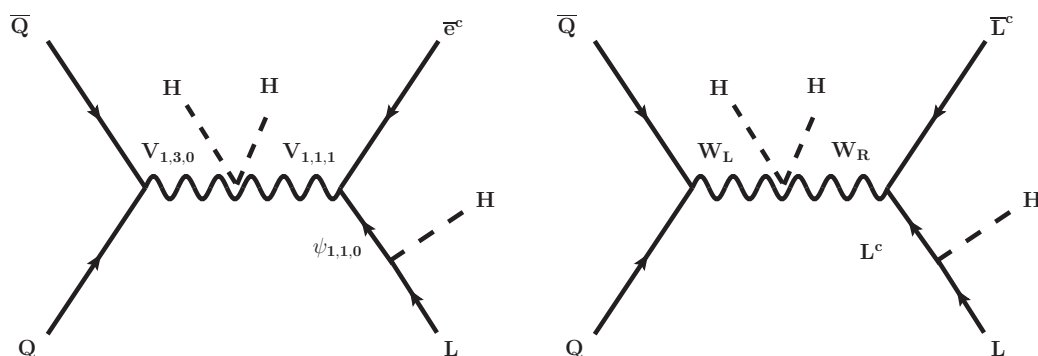


**Figure 7.**  $\mathcal{O}_7$   $d = 9$  contribution to  $0\nu\beta\beta$  decay decomposed as  $(\bar{Q}Q)(HH)(\bar{e}^c)(LH)$  in the SM (left) and in the LR model (right).

is the light neutrino mass. This, in general, is expected to be a small number of order  $\sum_{j=1}^3 U_{ej}V_{ej} \sim 10^{-5} \sqrt{(\frac{m_\nu}{0.1\text{eV}})(\frac{1\text{TeV}}{M_M})}$ . In this case one expects the mass mechanism to dominate over both  $\langle\lambda\rangle$  and  $\langle\eta\rangle$ , given current limits on  $W_L - W_R$  mixing [72] and lower limits on the  $W_R$  mass from LHC [73, 74]. However, as in the LQ example model discussed previously in section 3.1, contributions to the neutrino mass matrix contain a sum over the three heavy right-handed neutrinos. In the case of severe fine-tuning of the parameters entering the neutrino mass matrix, the connection between the light-heavy neutrino mixing and  $\langle m_\nu \rangle$  can be avoided, see section 3.1. In this particular part of parameter space, the incomplete  $\sum_{j=1}^3 U_{ej}V_{ej}$  could in principle be larger than the naive expectation. Recall that the current bound on non-unitarity of  $U$  is of the order of 1 % [54]. For  $\sum_{j=1}^3 U_{ej}V_{ej}$  as large as  $\sum_{j=1}^3 U_{ej}V_{ej} \sim \mathcal{O}(10^{-2})$   $\langle\lambda\rangle$  and/or  $\langle\eta\rangle$  could dominate over the mass mechanism, even after taking into account all other existing limits. We stress again that this is not the natural expectation.

In summary, there are some particular decompositions of  $d = 9$  operators containing the SM  $W$  or Higgs boson. In those cases the  $d = 9$  operator scales as  $1/(\Lambda^3 v_{\text{SM}}^2)$  and can be as important as the corresponding decomposition of the  $d = 7$  operator.

## 5 Summary

We have studied  $d = 7$   $\Delta L = 2$  operators and their relation with the long-range part of the amplitude for  $0\nu\beta\beta$  decay. We have given the complete list of decompositions for the relevant operators and discussed a classification scheme for these decompositions based on the level of perturbation theory, at which the different models produce neutrino masses. For tree-level and 1-loop neutrino mass models we expect that the mass mechanism is more important than the long-range ( $\not{p}$ -enhanced) amplitude. We have discussed how this conclusion may be avoided in highly fine-tuned regions in parameter space. For 2-loop neutrino mass models based on  $d = 7$  operators, the long-range amplitude usually is more important than the mass mechanism. To demonstrate this, we have discussed in some detail a model based on  $\mathcal{O}_8$ .

We also discussed the connection of our work with previously considered long-range contributions in left-right symmetric models. This served to point out some particularities about the operator classification, that we rely on, in cases where higher order operators, such as  $d = 9$  ( $\mathcal{O}_9 \propto \Lambda_{\text{LNV}}^{-5}$ ), are effectively reduced to lower order operators, i.e.  $d = 7$  ( $\mathcal{O}_9^{\text{eff}} \propto \Lambda_{\text{LNV}}^{-3} \times \Lambda_{\text{EW}}^{-2}$ ).

Our main results are summarized in tabular form in the appendix, where we give the complete list of possible models, which lead to contributions to the long-range part of the amplitude for  $0\nu\beta\beta$  decay. In particular, table 4 and table 5 contain several exotic possibilities not discussed in the literature before: models with vector-like fermions and vectors with exotic quantum numbers, such as  $V_{1,2,3/2}$ . From this list one can deduce, which contractions can lead to interesting phenomenology, i.e. models that are testable also at the LHC.

### Acknowledgments

M.H. thanks the Universidad Tecnica Federico Santa Maria, Valparaiso, for hospitality during his stay. M.H. is supported by the Spanish grants FPA2014-58183-P, SEV-2014-0398 and Multidark CSD2009-00064 (MINECO), and PROMETEOII/2014/084 (Generalitat Valenciana). J.C.H. is supported by Chile grants Fondecyt No. 1161463 and Conicyt ACT 1406. The research of T.O. is supported by JSPS Grants-in-Aid for Scientific Research on Innovative Areas *Unification and Development of the Neutrino Science Frontier* Number 2610 5503.

### A Decompositions of the long range $0\nu\beta\beta$ operators

Here we present the summary tables of all tree-level decompositions of the Babu-Leung operators #3 (table 3), #4 (table 4), and #8 (table 5) with mass dimension  $d = 7$ . The effective operators are decomposed into renormalizable interactions by assigning the fields to the outer legs of the tree diagram shown in figure 8. The assignments of the outer fields are shown at the ‘‘Decompositions’’ column, and the (inner) fields required by the corresponding decompositions are listed at the ‘‘Mediators’’ column. The symbols  $S$  and  $\psi$  represents the Lorentz nature of the mediators:  $S^{(\prime)}$  is a scalar field, and  $\psi_{L(R)}$  is a left(right)-handed fermion. The charges of the mediators under the SM gauge groups are identified and expressed with the format  $(\text{SU}(3)_c, \text{SU}(2)_L)_{\text{U}(1)_Y}$ . It is easy to find the contributions of the effective operators to neutrinoless double beta decay processes at the ‘‘Projection to the basis ops.’’ column. The basis operators are defined as

$$\begin{aligned} \mathcal{O}_{3a}(\alpha, \beta) &\equiv (i\tau^2)^{ij} (i\tau^2)^{kl} \{(\overline{L}_\alpha^c)_i^a (L_\beta)_{ja}\} \{(\overline{d}_R)^{Ib} (Q)_{Ikb}\} H_l \\ &\supset \frac{1}{4} \left[ j_{S+P}^\dagger(\alpha, \beta) - j_{S+P}^\dagger(\beta, \alpha) \right] J_{S+P}^\dagger H^0, \end{aligned} \tag{A.1}$$

$$\begin{aligned} \mathcal{O}_{3b}(\alpha, \beta) &\equiv (i\tau^2)^{ik} (i\tau^2)^{jl} \{(\overline{L}_\alpha^c)_i^a (L_\beta)_{ja}\} \{(\overline{d}_R)^{Ib} (Q)_{Ikb}\} H_l \\ &\supset -\frac{1}{4} j_{S+P}^\dagger(\beta, \alpha) J_{S+P}^\dagger H^0 + \frac{1}{4} \{\overline{\ell}_\alpha^c (1 - \gamma^5) \ell_\beta\} J_{S+P}^\dagger H^+, \end{aligned} \tag{A.2}$$

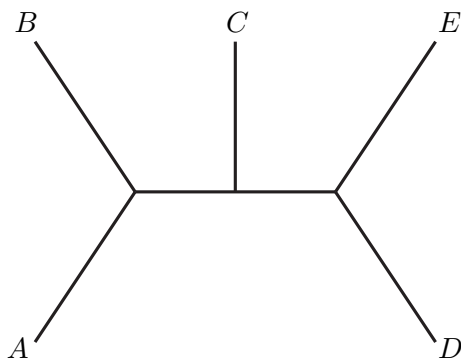


**Figure 8.** Topology for tree-level decompositions of Babu-Leung operator #3, #4, and #8. Once the SM fields,  $A, B, C, D$ , and  $E$ , are assigned to the outer legs, the Lorentz nature and the SM gauge charges of the mediation fields are uniquely determined. The assignments of the outer fields are expressed as  $(AB)(C)(DE)$  and listed at the “Decompositions” column in tables 3–5.

$$\begin{aligned} \mathcal{O}_{3a}^{\text{ten.}}(\alpha, \beta) &\equiv (i\tau^2)^{ij}(i\tau^2)^{kl}\{(\overline{L^c_\alpha})^a(\sigma^{\rho\sigma})_a{}^b(L_\beta)_{jb}\}\{(\overline{d_R})^{Ic}(\sigma_{\rho\sigma})_c{}^d(Q)_{Ikd}\}H_l \\ &\supset -\frac{1}{16}\left[(j_{T_R}^\dagger)^{\rho\sigma}(\alpha, \beta) + (j_{T_R}^\dagger)^{\rho\sigma}(\beta, \alpha)\right](J_{T_R}^\dagger)_{\rho\sigma}H^0, \end{aligned} \quad (\text{A.3})$$

$$\begin{aligned} \mathcal{O}_{3b}^{\text{ten.}}(\alpha, \beta) &\equiv (i\tau^2)^{ik}(i\tau^2)^{jl}\{(\overline{L^c_\alpha})^a(\sigma^{\rho\sigma})_a{}^b(L_\beta)_{jb}\}\{(\overline{d_R})^{Ic}(\sigma_{\rho\sigma})_c{}^d(Q)_{Ikd}\}H_l \\ &\supset -\frac{1}{16}(j_{T_R}^\dagger)^{\rho\sigma}(\beta, \alpha)(J_{T_R}^\dagger)_{\rho\sigma}H^0 - \frac{1}{16}\{\overline{\ell^c_\alpha}\gamma^{\rho\sigma}(1 - \gamma^5)\ell_\beta\}(J_{T_R}^\dagger)_{\rho\sigma}H^+, \end{aligned} \quad (\text{A.4})$$

$$\begin{aligned} \mathcal{O}_{4a}(\alpha, \beta) &\equiv (i\tau)^{jk}(\overline{L^c_\alpha})^a(L_\beta)_{ja}(\overline{Q})_{\dot{a}}^{Ii}(u_R)_{\dot{I}}^{\dot{a}}H_k \\ &\supset \frac{1}{4}J_{S+P}^\dagger(\beta, \alpha)J_{S-P}^\dagger H^0 - \frac{1}{4}\overline{\ell^c_\alpha}(1 - \gamma^5)\ell_\beta J_{S-P}^\dagger H^+, \end{aligned} \quad (\text{A.5})$$

$$\begin{aligned} \mathcal{O}_{4b}(\alpha, \beta) &\equiv (i\tau^2)^{ij}(\overline{L^c_\alpha})^a(L_\beta)_{ja}(\overline{Q})_{\dot{a}}^{Ik}(u_R)_{\dot{I}}^{\dot{a}}H_k \\ &\supset \frac{1}{4}\left[j_{S+P}^\dagger(\alpha, \beta) - j_{S+P}^\dagger(\beta, \alpha)\right]J_{S-P}^\dagger H^0, \end{aligned} \quad (\text{A.6})$$

$$\begin{aligned} \mathcal{O}_8(\alpha, \beta) &\equiv (\overline{L^c_\alpha})^a(\sigma^\rho)_{a\dot{a}}(e_{R\beta})^{\dot{a}}(\overline{d_R})^{Ib}(\sigma_\rho)_{\dot{b}b}(u_R)_{\dot{I}}^{\dot{b}}(i\tau^2)^{ij}H_j \\ &\supset \frac{1}{4}(j_{V+A}^\dagger)^\rho(J_{V+A}^\dagger)_\rho H^0 - \frac{1}{4}\{\overline{\ell^c_\alpha}\gamma^\rho(1 + \gamma^5)\ell_\beta\}(J_{V+A}^\dagger)_\rho H^+. \end{aligned} \quad (\text{A.7})$$

Here we explicitly write all the indices:  $\alpha, \beta$  for lepton flavour, the lower (upper)  $I$  for  $\mathbf{3}$  ( $\overline{\mathbf{3}}$ ) of SU(3) colour,  $i, j, k, l$  for  $\mathbf{2}$  of SU(2) left,  $\rho, \sigma$  for Lorentz vector, and  $a, b, c, d$  ( $\dot{a}, \dot{b}$ ) for left(right)-handed Lorentz spinor. The lowest-loop contributions (i.e., dominant contributions) to neutrino masses are found at the columns “ $m_\nu$ ”. We are mainly interested in decompositions (=proto-models) where new physics contributions to  $0\nu\beta\beta$  can compete with the mass mechanism contribution mediated by the effective neutrino mass  $\langle m_\nu \rangle$ . An annotation “w. (additional interaction)” is given in the column of “ $m_\nu$ @1loop” for some decompositions. This shows that one can draw the 1-loop diagram, putting the interactions that appear in the decomposition and *the additional interaction* together. The additional interactions given in the tables are not included in the decomposition but are not forbidden by the SM gauge symmetries, nor can they be eliminated by any (abelian) discrete



symmetry, without removing at least some of the interactions present in the decomposition. For example, using the interactions appear in decomposition #11 of Babu-Leung operator #8 (see table 5), one can construct two 2-loop neutrino mass diagrams mediated by the Nambu-Goldstone boson  $H^+$ , whose topologies are  $T2_2^B$  and  $T2_4^B$  of [64]. This also corresponds to the 2-loop neutrino mass model labelled with  $\mathcal{O}_8^1$  in [40]. However, to regularize the divergence in diagram  $T2_4^B$ , the additional interaction  $(\overline{Q^c})_{Ii}^a (i\tau^2)^{ij} (L)_{ia} S^I$  is necessary, and this interaction generates a 1-loop neutrino mass diagram. Consequently, this decomposition should be regarded as a 1-loop neutrino mass model.<sup>8</sup> We also show the 1-loop neutrino mass models that require an additional interaction with an additional field (second Higgs doublet  $H'$ ) with bracket.<sup>9</sup>

The two contributions to  $0\nu\beta\beta$  are compared in section 3 with some concrete examples. The comparison is summarized at table 2. In short, the mass mechanism dominates  $0\nu\beta\beta$  if neutrino masses are generated at the tree or the 1-loop level. When neutrino masses are generated from 2-loop diagrams, new physics contributions to  $0\nu\beta\beta$  become comparable with the mass mechanism contribution and can be large enough to be within reach of the sensitivities of next generation experiments. However, the 2-loop neutrino masses generated from the decompositions of the Babu-Leung operators of #3 and #4 are anti-symmetric with respect to the flavour indices, such as the original Zee model and, thus, are already excluded by oscillation experiments. Therefore, if we adopt those decompositions as neutrino mass models, we must extend the models to make the neutrino masses compatible with oscillation data. In such models, the extension part controls the mass mechanism contribution and also the new physics contribution to  $0\nu\beta\beta$ , and consequently, we cannot compare the contributions without a full description of the models including the extension. Nonetheless, it might be interesting to point out that decomposition #8 of the Babu-Leung #3 contains the tensor operator  $\mathcal{O}_{3a}^{\text{ten}}(e, e)$ , which gives a contribution to  $0\nu\beta\beta$  and generates neutrino masses with the  $(e, e)$  component at the two-loop level. On the other hand, 2-loop neutrino mass models inspired by decompositions of Babu-Leung #8 possess a favourable flavour structure. This possibility has been investigated in section 3.3 with a concrete example.

Note that reference [40] gives the decompositions for the  $d=7$  operators, but does not discuss long-range double beta decay. The long-range contribution [69] in left-right symmetric models [37–39] corresponds to decomposition #14 in table 5. The leptoquark mechanism [36] is encoded in decomposition #2 in tables 3 and 4, as well as decompositions #2 and #3 in table 5. Further references to models studied previously in the literature are given in the tables.

There is another category of lepton-number-violating effective operators, not contained in the catalogue by Babu and Leung: operators with covariant derivatives  $D_\rho$ . These

---

<sup>8</sup>We note that the same argument holds for all decompositions containing the scalar  $S_{3,1,1/3}$  listed in [27] as 2-loop  $d = 7$  models.

<sup>9</sup>Although the interaction  $(\partial_\rho H)_i (i\tau^2)^{ij} H_j V^\rho$  listed in table 5 can be constructed only with the SM Higgs doublets  $H$  and the vector mediator  $V$  of the  $d = 7$  operator, the interaction does not appear in the models where the vector mediator  $V$  is the gauge boson of an extra gauge symmetry. However, if we allow the introduction of an additional Higgs doublet  $H'$ , we can have the  $(\partial_\rho H)_i H'^{\dagger i} V^\rho$  through the mixing between  $H$  and  $H'$ .

Eff. op.	Decom.	$(m_\nu)_{\alpha\beta}$	$\Lambda_7$ [GeV] suggested by $m_\nu = 0.05$ eV	$\mathcal{A}^{\text{MM}}/\mathcal{A}^{\text{LR}}$
$LL\bar{d}_R QH$	#1,3,4,5,6,9	$\frac{v^2}{\Lambda}$	$\sim 10^{15}$	$\frac{\Lambda^2}{p_F v} \sim 10^{28}$
	#2,7,8	$\frac{y_b}{16\pi^2} \frac{v^2}{\Lambda}$	$\sim 10^{11}$	$\frac{y_b}{16\pi^2} \frac{\Lambda^2}{p_F v} \sim 10^{17}$
	[#1, 3, 5, 8	$\frac{y_b g^2}{(16\pi^2)^2} \frac{v^2}{\Lambda} (\alpha \neq \beta)$	$\sim 10^8$	$\frac{y_b g^2}{(16\pi^2)^2} \frac{\Lambda^2}{p_F v} \sim 10^9]$
$LL\bar{Q}u_R H$	#1,3,4,5,6,8,9	$\frac{v^2}{\Lambda}$	$\sim 10^{15}$	$\frac{\Lambda^2}{p_F v} \sim 10^{28}$
	#2,7,8	$\frac{y_t}{16\pi^2} \frac{v^2}{\Lambda}$	$\sim 10^{12}$	$\frac{y_t}{16\pi^2} \frac{\Lambda^2}{p_F v} \sim 10^{21}$
	[#1, 3, 5, 8	$\frac{y_t g^2}{(16\pi^2)^2} \frac{v^2}{\Lambda} (\alpha \neq \beta)$	$\sim 10^{10}$	$\frac{y_t g^2}{(16\pi^2)^2} \frac{\Lambda^2}{p_F v} \sim 10^{14}]$
$Le_R\bar{d}_R u_R H$	#5,8,14	$\frac{v^2}{\Lambda}$	$\sim 10^{15}$	$\frac{\Lambda^2}{p_F v} \sim 10^{28}$
	#2,12	$\frac{y_t}{16\pi^2} \frac{v^2}{\Lambda}$	$\sim 10^{12}$	$\frac{y_t}{16\pi^2} \frac{\Lambda^2}{p_F v} \sim 10^{21}$
	#3,11	$\frac{y_b}{16\pi^2} \frac{v^2}{\Lambda}$	$\sim 10^{11}$	$\frac{y_b}{16\pi^2} \frac{\Lambda^2}{p_F v} \sim 10^{17}$
	#1,4,6,7,9, 10,13,15	$y_{\ell\beta} \frac{y_b y_t g^2}{(16\pi^2)^2} \frac{v^4}{\Lambda^3}$	$\sim 10^3 (\beta = \tau)$	$y_e \frac{y_b y_t g^2}{(16\pi^2)^2} \frac{v}{p_F} \sim 10^{-9}$

**Table 2.** Comparison between the amplitude  $\mathcal{A}^{\text{LR}}$  of new physics long-range contributions to  $0\nu\beta\beta$  and that  $\mathcal{A}^{\text{MM}}$  of the mass mechanism. When the neutrino mass is generated at the tree and one-loop level, the new physics scale  $\Lambda_7$  must be sufficiently high to reproduce the correct size of neutrino masses, consequently, the long-range contributions  $\mathcal{A}^{\text{LR}}$  are suppressed and the mass mechanism dominates the contribution to  $0\nu\beta\beta$ . As usual in such operator analysis, these estimates do not take into account that some non-SM Yukawa couplings, appearing in the ultra-violet completion of the operators, could be sizably smaller than one, which would lead to lower scales  $\Lambda_7$ . Also, for loop model the scales could be overestimated, since they neglect loop integrals. The neutrino masses generated at the two-loop level from the decompositions of the Babu-Leung #8 operator should be estimated with  $d = 7$   $LLHHH^\dagger$  operator (as illustrated in section 3.3). In addition, they receive additional suppression from the lepton Yukawa coupling  $y_{\ell\beta}$ , which further lowers the new physics scale  $\Lambda_7$ . Note that in particular for the 2-loop  $d = 7$  models, as the concrete example in section 3.3 shows, the estimate for  $\mathcal{A}^{\text{MM}}/\mathcal{A}^{\text{LR}}$  can vary by several orders of magnitude, depending on parameters. However, both the estimate shown here and the explicit calculation in section 3.3 give numbers  $\mathcal{A}^{\text{MM}}/\mathcal{A}^{\text{LR}} \ll 1$ , such that the long-range contribution dominates always over the mass mechanism for these decompositions.

have been intensively studied in refs. [41, 42, 55]. The derivative operators with mass dimension seven are classified into two types by their ingredient fields; one is  $D_\rho D^\rho LLHH$  and the other is  $D_\rho L\gamma^\rho e_R HHH$ . With the full decomposition, it is straightforward to show that the tree-level decompositions of the first type must contain one of the seesaw mediators. Therefore, the neutrino masses are generated at the tree level and the mass mechanism always dominate the contributions to  $0\nu\beta\beta$ . The decompositions of the second type also require the scalar triplet of the type II seesaw mechanism when we do not employ vector fields as mediators, and the new physics contributions to  $0\nu\beta\beta$  become insignificant again compared to the mass mechanism. In ref. [55], the authors successfully obtained the derivative operator  $(\bar{e}_R^c \gamma^\rho L i \tau^2 \vec{\tau} \vec{W}_\rho H')(H i \tau^2 H')$  at the tree level and simultaneously

#	Decompositions	Mediators	Projection to the basis ops.	$m_\nu$ @tree	$m_\nu$ @1loop	$m_\nu$ @2loop	
#1	$(L_\alpha L_\beta)(H)(\bar{d}_R Q)$	$S(\mathbf{1}, \mathbf{1})_{+1}$	$S'(\mathbf{1}, \mathbf{2})_{+\frac{1}{2}}$	$-\mathcal{O}_{3a}(\alpha, \beta)$	—	TvI-ii w. $\bar{\ell}_R L S'^\dagger$	$T2_4^B(\alpha \neq \beta)$ $\mathcal{O}_3^2$ in [40]
		$S(\mathbf{1}, \mathbf{3})_{+1}$	$S'(\mathbf{1}, \mathbf{2})_{+\frac{1}{2}}$	$-\mathcal{O}_{3b}(\alpha, \beta) - \mathcal{O}_{3b}(\beta, \alpha)$	type II		
#2	$(L_\alpha Q)(H)(\bar{d}_R L_\beta)$	$S(\bar{\mathbf{3}}, \mathbf{1})_{+\frac{1}{3}}$	$S'(\bar{\mathbf{3}}, \mathbf{2})_{-\frac{1}{6}}$	$\frac{1}{2}\mathcal{O}_{3b}(\alpha, \beta) - \frac{1}{2}\mathcal{O}_{3b}^{\text{ten.}}(\alpha, \beta)$	—	TvI-ii [58] $\mathcal{O}_3^8$ in [40]	[15, 75]
		$S(\bar{\mathbf{3}}, \mathbf{3})_{+\frac{1}{3}}$	$S'(\bar{\mathbf{3}}, \mathbf{2})_{-\frac{1}{6}}$	$\frac{1}{2}\mathcal{O}_{3a}(\alpha, \beta) - \frac{1}{2}\mathcal{O}_{3a}^{\text{ten.}}(\alpha, \beta)$ $-\frac{1}{2}\mathcal{O}_{3b}(\beta, \alpha) - \frac{1}{2}\mathcal{O}_{3b}^{\text{ten.}}(\beta, \alpha)$	—	TvI-ii [58] $\mathcal{O}_3^9$ in [40]	[15]
#3	$(L_\alpha L_\beta)(Q)(\bar{d}_R H)$	$S(\mathbf{1}, \mathbf{1})_{+1}$	$\psi_{L,R}(\mathbf{3}, \mathbf{2})_{-\frac{5}{6}}$	$-\mathcal{O}_{3a}(\alpha, \beta)$	—	$\left[ \begin{array}{l} \text{TvI-ii} \\ \text{w. } S^\dagger H H' \end{array} \right]$	$T2_1^B(\alpha \neq \beta)$ $\mathcal{O}_3^1$ in [40]
		$S(\mathbf{1}, \mathbf{3})_{+1}$	$\psi_{L,R}(\mathbf{3}, \mathbf{2})_{-\frac{5}{6}}$	$-\mathcal{O}_{3b}(\alpha, \beta) - \mathcal{O}_{3b}(\beta, \alpha)$	type II		
#4	$(L_\alpha H)(Q)(\bar{d}_R L_\beta)$	$\psi_R(\mathbf{1}, \mathbf{1})_0$	$S(\bar{\mathbf{3}}, \mathbf{2})_{-\frac{1}{6}}$	$\frac{1}{2}\mathcal{O}_{3b}(\beta, \alpha) + \frac{1}{2}\mathcal{O}_{3b}^{\text{ten.}}(\beta, \alpha)$	type I		
		$\psi_R(\mathbf{1}, \mathbf{3})_0$	$S(\bar{\mathbf{3}}, \mathbf{2})_{-\frac{1}{6}}$	$-\frac{1}{2}\mathcal{O}_{3a}(\alpha, \beta) + \frac{1}{2}\mathcal{O}_{3a}^{\text{ten.}}(\alpha, \beta)$ $-\frac{1}{2}\mathcal{O}_{3b}(\alpha, \beta) + \frac{1}{2}\mathcal{O}_{3b}^{\text{ten.}}(\alpha, \beta)$	type III		
#5	$(L_\alpha L_\beta)(\bar{d}_R)(QH)$	$S(\mathbf{1}, \mathbf{1})_{+1}$	$\psi_{L,R}(\mathbf{3}, \mathbf{1})_{+\frac{2}{3}}$	$\mathcal{O}_{3a}(\alpha, \beta)$	—	$\left[ \begin{array}{l} \text{TvI-ii} \\ \text{w. } S^\dagger H H' \end{array} \right]$	$T2_2^B(\alpha \neq \beta)$ $\mathcal{O}_3^2$ in [40]
		$S(\mathbf{1}, \mathbf{3})_{+1}$	$\psi_{L,R}(\mathbf{3}, \mathbf{3})_{+\frac{2}{3}}$	$-\mathcal{O}_{3b}(\alpha, \beta) - \mathcal{O}_{3b}(\beta, \alpha)$	type II		
#6	$(L_\alpha Q)(\bar{d}_R)(L_\beta H)$	$S(\bar{\mathbf{3}}, \mathbf{1})_{+\frac{1}{3}}$	$\psi_R(\mathbf{1}, \mathbf{1})_0$	$-\frac{1}{2}\mathcal{O}_{3b}(\alpha, \beta) + \frac{1}{2}\mathcal{O}_{3b}^{\text{ten.}}(\alpha, \beta)$	type I		
		$S(\bar{\mathbf{3}}, \mathbf{3})_{+\frac{1}{3}}$	$\psi_R(\mathbf{1}, \mathbf{3})_0$	$\frac{1}{2}\mathcal{O}_{3a}(\alpha, \beta) - \frac{1}{2}\mathcal{O}_{3a}^{\text{ten.}}(\alpha, \beta)$ $-\frac{1}{2}\mathcal{O}_{3b}(\beta, \alpha) - \frac{1}{2}\mathcal{O}_{3b}^{\text{ten.}}(\beta, \alpha)$	type III		
#7	$(L_\alpha Q)(L_\beta)(\bar{d}_R H)$	$S(\bar{\mathbf{3}}, \mathbf{1})_{+\frac{1}{3}}$	$\psi_{L,R}(\mathbf{3}, \mathbf{2})_{-\frac{5}{6}}$	$\frac{1}{2}\mathcal{O}_{3b}(\alpha, \beta) - \frac{1}{2}\mathcal{O}_{3b}^{\text{ten.}}(\alpha, \beta)$	—	TvI-iii $\mathcal{O}_3^4$ in [40]	
		$S(\bar{\mathbf{3}}, \mathbf{3})_{+\frac{1}{3}}$	$\psi_{L,R}(\mathbf{3}, \mathbf{2})_{-\frac{5}{6}}$	$\frac{1}{2}\mathcal{O}_{3a}(\alpha, \beta) - \frac{1}{2}\mathcal{O}_{3a}^{\text{ten.}}(\alpha, \beta)$ $-\frac{1}{2}\mathcal{O}_{3b}(\beta, \alpha) - \frac{1}{2}\mathcal{O}_{3b}^{\text{ten.}}(\beta, \alpha)$	—	TvI-iii $\mathcal{O}_3^5$ in [40]	
#8	$(\bar{d}_R L_\alpha)(L_\beta)(QH)$	$S(\mathbf{3}, \mathbf{2})_{+\frac{1}{6}}$	$\psi_{L,R}(\mathbf{3}, \mathbf{1})_{+\frac{2}{3}}$	$-\frac{1}{2}\mathcal{O}_{3a}(\alpha, \beta) - \frac{1}{2}\mathcal{O}_{3a}^{\text{ten.}}(\alpha, \beta)$	—	—	$T2_2^B(m_\nu)_{\alpha \neq \beta}$ $\mathcal{O}_3^3$ in [40], [48]
		$S(\mathbf{3}, \mathbf{2})_{+\frac{1}{6}}$	$\psi_{L,R}(\mathbf{3}, \mathbf{3})_{+\frac{2}{3}}$	$\frac{1}{2}\mathcal{O}_{3b}(\alpha, \beta) + \frac{1}{2}\mathcal{O}_{3b}^{\text{ten.}}(\alpha, \beta)$ $+\frac{1}{2}\mathcal{O}_{3b}(\beta, \alpha) - \frac{1}{2}\mathcal{O}_{3b}^{\text{ten.}}(\beta, \alpha)$	—	TvI-iii $\mathcal{O}_3^6$ in [40]	
#9	$(L_\alpha H)(L_\beta)(\bar{d}_R Q)$	$\psi_R(\mathbf{1}, \mathbf{1})_0$	$S(\mathbf{1}, \mathbf{2})_{+\frac{1}{2}}$	$\mathcal{O}_{3b}(\beta, \alpha)$	type I		
		$\psi_R(\mathbf{1}, \mathbf{3})_0$	$S(\mathbf{1}, \mathbf{2})_{+\frac{1}{2}}$	$\mathcal{O}_{3a}(\alpha, \beta) + \mathcal{O}_{3b}(\alpha, \beta)$	type III		

**Table 3.** Decompositions and projections of the  $LL\bar{d}_R QH$  operator. New physics contributions to  $0\nu 2\beta$  are given as the combinations of the basis operators in the ‘‘Projection to the basis ops.’’ column. The tensor operators  $\mathcal{O}^{\text{ten.}}$  play an important role in the long-range contribution. The long-range contribution in R-parity violating SUSY models corresponds to decomposition #2 [34, 35].

#	Decompositions	Mediators	Projection to the basis ops.	$m_\nu$ @tree	$m_\nu$ @1loop	$m_\nu$ @2loop	
#1	$(L_\alpha L_\beta)(H)(\bar{Q}u_R)$	$S(\mathbf{1}, \mathbf{1})_{+1}$	$S'(\mathbf{1}, \mathbf{2})_{+\frac{1}{2}}$	$-\mathcal{O}_{4b}(\alpha, \beta)$	—	TvI-ii w. $\bar{e}_R L S^\dagger$	$T2_4^B(\alpha \neq \beta)$ $\mathcal{O}_4^3$ in [40]
		$S(\mathbf{1}, \mathbf{3})_{+1}$	$S'(\mathbf{1}, \mathbf{2})_{+\frac{1}{2}}$	$\mathcal{O}_{4a}(\alpha, \beta) + \mathcal{O}_{4a}(\beta, \alpha)$	type II		
#2	$(\bar{Q}L_\alpha)(H)(L_\beta u_R)$	$V(\mathbf{3}, \mathbf{1})_{+\frac{2}{3}}$	$V'(\mathbf{3}, \mathbf{2})_{+\frac{1}{6}}$	$2\mathcal{O}_{4a}(\alpha, \beta)$	—	TvI-ii	
		$V(\mathbf{3}, \mathbf{3})_{+\frac{2}{3}}$	$V'(\mathbf{3}, \mathbf{2})_{+\frac{1}{6}}$	$2\mathcal{O}_{4a}(\beta, \alpha) - 2\mathcal{O}_{4b}(\alpha, \beta)$	—	TvI-ii	
#3	$(L_\alpha L_\beta)(\bar{Q})(u_R H)$	$S(\mathbf{1}, \mathbf{1})_{+1}$	$\psi_{L,R}(\mathbf{3}, \mathbf{2})_{+\frac{7}{6}}$	$\mathcal{O}_{4b}(\alpha, \beta)$	—	$\left[ \begin{array}{l} \text{TvI-ii} \\ \text{w. } S^\dagger H H' \end{array} \right]$	$T2_1^B(\alpha \neq \beta)$ $\mathcal{O}_4^3$ in [40]
		$S(\mathbf{1}, \mathbf{3})_{+1}$	$\psi_{L,R}(\mathbf{3}, \mathbf{2})_{+\frac{7}{6}}$	$\mathcal{O}_{4a}(\alpha, \beta) + \mathcal{O}_{4a}(\beta, \alpha)$	type II		
#4	$(L_\alpha H)(\bar{Q})(L_\beta u_R)$	$\psi_R(\mathbf{1}, \mathbf{1})_0$	$V(\mathbf{3}, \mathbf{2})_{+\frac{1}{6}}$	$2\mathcal{O}_{4a}(\beta, \alpha)$	type I		
		$\psi_R(\mathbf{1}, \mathbf{3})_0$	$V(\mathbf{3}, \mathbf{2})_{+\frac{1}{6}}$	$-2\mathcal{O}_{4a}(\alpha, \beta) + 2\mathcal{O}_{4b}(\alpha, \beta)$	type III		
#5	$(L_\alpha L_\beta)(u_R)(\bar{Q}H)$	$S(\mathbf{1}, \mathbf{1})_{+1}$	$\psi_{L,R}(\bar{\mathbf{3}}, \mathbf{1})_{+\frac{1}{3}}$	$\mathcal{O}_{4b}(\alpha, \beta)$	—	$\left[ \begin{array}{l} \text{TvI-ii} \\ \text{w. } S^\dagger H H' \end{array} \right]$	$T2_2^B(\alpha \neq \beta)$ $\mathcal{O}_4^2$ in [40]
		$S(\mathbf{1}, \mathbf{3})_{+1}$	$\psi_{L,R}(\bar{\mathbf{3}}, \mathbf{3})_{+\frac{1}{3}}$	$\mathcal{O}_{4a}(\alpha, \beta) + \mathcal{O}_{4a}(\beta, \alpha)$	type II		
#6	$(\bar{Q}L_\alpha)(u_R)(L_\beta H)$	$V(\mathbf{3}, \mathbf{1})_{+\frac{2}{3}}$	$\psi_R(\mathbf{1}, \mathbf{1})_0$	$2\mathcal{O}_{4a}(\alpha, \beta)$	type I		
		$V(\mathbf{3}, \mathbf{3})_{+\frac{2}{3}}$	$\psi_R(\mathbf{1}, \mathbf{3})_0$	$-2\mathcal{O}_{4b}(\alpha, \beta) - 2\mathcal{O}_{4a}(\beta, \alpha)$	type III		
#7	$(\bar{Q}L_\alpha)(L_\beta)(u_R H)$	$V(\mathbf{3}, \mathbf{1})_{+\frac{2}{3}}$	$\psi_{L,R}(\mathbf{3}, \mathbf{2})_{+\frac{7}{6}}$	$-2\mathcal{O}_{4a}(\alpha, \beta)$	—	TvI-iii	
		$V(\mathbf{3}, \mathbf{3})_{+\frac{2}{3}}$	$\psi_{L,R}(\mathbf{3}, \mathbf{2})_{+\frac{7}{6}}$	$2\mathcal{O}_{4b}(\alpha, \beta) + 2\mathcal{O}_{4a}(\beta, \alpha)$	—	TvI-iii	
#8	$(Lu_R)(L)(\bar{Q}H)$	$V(\bar{\mathbf{3}}, \mathbf{2})_{-\frac{1}{6}}$	$\psi_{L,R}(\mathbf{3}, \mathbf{1})_{-\frac{1}{3}}$	$2\mathcal{O}_{4b}(\alpha, \beta)$	—	—	$T2_2^B(\alpha \neq \beta)$
		$V(\bar{\mathbf{3}}, \mathbf{2})_{-\frac{1}{6}}$	$\psi_{L,R}(\mathbf{3}, \mathbf{3})_{-\frac{1}{3}}$	$2\mathcal{O}_{4a}(\alpha, \beta) + 2\mathcal{O}_{4a}(\beta, \alpha)$	—	TvI-iii	
#9	$(LH)(L)(\bar{Q}u_R)$	$\psi_R(\mathbf{1}, \mathbf{1})_0$	$S(\mathbf{1}, \mathbf{2})_{+\frac{1}{2}}$	$-\mathcal{O}_{4a}(\beta, \alpha)$	type I		
		$\psi_R(\mathbf{1}, \mathbf{3})_0$	$S(\mathbf{1}, \mathbf{2})_{+\frac{1}{2}}$	$-\mathcal{O}_{4a}(\alpha, \beta) + \mathcal{O}_{4b}(\alpha, \beta)$	type III		

**Table 4.** Decomposition and projection of the  $LL\bar{Q}u_R H$  operator.

#	Decompositions	Mediators		Projection to the basis ops.	$m_\nu$ @tree	$m_\nu$ @1loop	$m_\nu$ @2loop
#1	$(L_\alpha e_{R\beta})(H)(\overline{d}_R u_R)$	$V(\mathbf{1}, \mathbf{2})_{+\frac{3}{2}}$	$V'(\mathbf{1}, \mathbf{1})_{-1}$	$\mathcal{O}_8(\alpha, \beta)$	—	$\left[ \begin{array}{l} \text{T}\nu\text{I-i} \\ \text{w. } \partial H H V' \end{array} \right]$	$2 \times T_4^{\text{B}}$
#2	$(L_\alpha u_R)(H)(\overline{d}_R e_{R\beta})$	$V(\overline{\mathbf{3}}, \mathbf{2})_{-\frac{1}{6}}$	$V'(\overline{\mathbf{3}}, \mathbf{1})_{-\frac{2}{3}}$	$\mathcal{O}_8(\alpha, \beta)$	—	$\begin{array}{l} \text{T}\nu\text{I-ii} \\ \text{w. } \overline{Q} L V^\dagger \end{array}$	$T_2^{\text{B}} + T_4^{\text{B}}$
#3	$(\overline{d}_R L_\alpha)(H)(u_R e_{R\beta})$	$S(\mathbf{3}, \mathbf{2})_{+\frac{1}{6}}$	$S'(\mathbf{3}, \mathbf{1})_{-\frac{1}{3}}$	$\frac{1}{2}\mathcal{O}_8(\alpha, \beta)$	—	$\begin{array}{l} \text{T}\nu\text{I-ii} \\ \text{w. } Q L S^\dagger \end{array}$	$T_2^{\text{B}} + T_4^{\text{B}}$ $\mathcal{O}_8^4$ in [40], [75]
#4	$(L_\alpha e_{R\beta})(u_R)(\overline{d}_R H)$	$V(\mathbf{1}, \mathbf{2})_{+\frac{3}{2}}$	$\psi_{L,R}(\mathbf{3}, \mathbf{2})_{-\frac{5}{6}}$	$\mathcal{O}_8(\alpha, \beta)$	—	—	$T_1^{\text{B}} + T_2^{\text{B}}$
#5	$(L_\alpha H)(u_R)(\overline{d}_R e_{R\beta})$	$\psi_R(\mathbf{1}, \mathbf{1})_0$	$V(\overline{\mathbf{3}}, \mathbf{1})_{-\frac{2}{3}}$	$\mathcal{O}_8(\alpha, \beta)$	type I	—	—
#6	$(\overline{d}_R L_\alpha)(u_R)(e_{R\beta} H)$	$S(\mathbf{3}, \mathbf{2})_{+\frac{1}{6}}$	$\psi_{L,R}(\mathbf{1}, \mathbf{2})_{-\frac{1}{2}}$	$\frac{1}{2}\mathcal{O}_8(\alpha, \beta)$	—	—	$T_1^{\text{B}} + T_2^{\text{B}}$ $\mathcal{O}_8^2$ in [40]
#7	$(L_\alpha e_{R\beta})(\overline{d}_R)(u_R H)$	$V(\mathbf{1}, \mathbf{2})_{+\frac{3}{2}}$	$\psi_{L,R}(\mathbf{3}, \mathbf{2})_{+\frac{7}{6}}$	$\mathcal{O}_8(\alpha, \beta)$	—	—	$T_1^{\text{B}} + T_2^{\text{B}}$
#8	$(L_\alpha H)(\overline{d}_R)(u_R e_{R\beta})$	$\psi_R(\mathbf{1}, \mathbf{1})_0$	$S(\mathbf{3}, \mathbf{1})_{-\frac{1}{3}}$	$\frac{1}{2}\mathcal{O}_8(\alpha, \beta)$	type I	—	—
#9	$(L_\alpha u_R)(\overline{d}_R)(e_{R\beta} H)$	$V(\overline{\mathbf{3}}, \mathbf{2})_{-\frac{1}{6}}$	$\psi_{L,R}(\mathbf{1}, \mathbf{2})_{-\frac{1}{2}}$	$\mathcal{O}_8(\alpha, \beta)$	—	—	$T_1^{\text{B}} + T_2^{\text{B}}$
#10	$(e_{R\beta} H)(L_\alpha)(\overline{d}_R u_R)$	$\psi_{L,R}(\mathbf{1}, \mathbf{2})_{+\frac{1}{2}}$	$V(\mathbf{1}, \mathbf{1})_{+1}$	$-\mathcal{O}_8(\alpha, \beta)$	—	$\left[ \begin{array}{l} \text{T}\nu\text{I-ii} \\ \text{w. } \partial H H V \end{array} \right]$	$2 \times T_4^{\text{B}}$
#11	$(e_{R\beta} u_R)(L_\alpha)(\overline{d}_R H)$	$S(\overline{\mathbf{3}}, \mathbf{1})_{+\frac{1}{3}}$	$\psi_{L,R}(\mathbf{3}, \mathbf{2})_{-\frac{5}{6}}$	$-\frac{1}{2}\mathcal{O}_8(\alpha, \beta)$	—	$\begin{array}{l} \text{T}\nu\text{I-iii} \\ \text{w. } Q L S \end{array}$	$T_2^{\text{B}} + T_4^{\text{B}}$ $\mathcal{O}_8^1$ in [40]
#12	$(\overline{d}_R e_{R\beta})(L_\alpha)(u_R H)$	$V(\mathbf{3}, \mathbf{1})_{+\frac{2}{3}}$	$\psi_{L,R}(\mathbf{3}, \mathbf{2})_{+\frac{7}{6}}$	$\mathcal{O}_8(\alpha, \beta)$	—	$\begin{array}{l} \text{T}\nu\text{I-iii} \\ \text{w. } \overline{Q} L V \end{array}$	$T_2^{\text{B}} + T_4^{\text{B}}$
#13	$(L_\alpha u_R)(e_{R\beta})(\overline{d}_R H)$	$V(\overline{\mathbf{3}}, \mathbf{2})_{-\frac{1}{6}}$	$\psi_{L,R}(\mathbf{3}, \mathbf{2})_{-\frac{5}{6}}$	$-\mathcal{O}_8(\alpha, \beta)$	—	—	$2 \times T_2^{\text{B}}$
#14	$(L_\alpha H)(e_{R\beta})(\overline{d}_R u_R)$	$\psi_R(\mathbf{1}, \mathbf{1})_0$	$V(\mathbf{1}, \mathbf{1})_{+1}$	$\mathcal{O}_8(\alpha, \beta)$	type I	—	—
#15	$(\overline{d}_R L_\alpha)(e_{R\beta})(u_R H)$	$S(\overline{\mathbf{3}}, \mathbf{2})_{+\frac{1}{6}}$	$\psi_{L,R}(\mathbf{3}, \mathbf{2})_{+\frac{7}{6}}$	$\frac{1}{2}\mathcal{O}_8(\alpha, \beta)$	—	—	$2 \times T_2^{\text{B}}$ $\mathcal{O}_8^3$ in [40]

**Table 5.** Decomposition of the  $L e_R u_R \overline{d}_R H$  operator. The long-range contribution [69] in left-right symmetric models [37–39] corresponds to decomposition #14 .

avoided the tree-level neutrino mass with the help of a second Higgs doublet  $H'(\mathbf{1}, \mathbf{2})_{+1/2}$  and a  $Z_2$  parity which is broken spontaneously. Here we restrict ourselves to use the ingredients obtained from decompositions and do not discuss such extensions. Within our framework, the derivative operators are always associated with tree-level neutrino masses. In this study, we have mainly focused on the cases where the new physics contributions give a considerable impact on the  $0\nu\beta\beta$  processes. Therefore, we do not go into the details of the decompositions of the derivative operators.

**Open Access.** This article is distributed under the terms of the Creative Commons Attribution License ([CC-BY 4.0](https://creativecommons.org/licenses/by/4.0/)), which permits any use, distribution and reproduction in any medium, provided the original author(s) and source are credited.

## References

- [1] F.F. Deppisch, M. Hirsch and H. Pas, *Neutrinoless double beta decay and physics beyond the standard model*, *J. Phys. G* **39** (2012) 124007 [[arXiv:1208.0727](https://arxiv.org/abs/1208.0727)] [[INSPIRE](#)].
- [2] M. Hirsch, *Theoretical implications of  $0\nu\beta\beta$  decay measurements*, *AIP Conf. Proc.* **1666** (2015) 170007 [[INSPIRE](#)].
- [3] J. Schechter and J.W.F. Valle, *Neutrinoless double beta decay in  $SU(2) \times U(1)$  theories*, *Phys. Rev. D* **25** (1982) 2951 [[INSPIRE](#)].
- [4] M. Duerr, M. Lindner and A. Merle, *On the quantitative impact of the Schechter-Valle theorem*, *JHEP* **06** (2011) 091 [[arXiv:1105.0901](https://arxiv.org/abs/1105.0901)] [[INSPIRE](#)].
- [5] D.V. Forero, M. Tortola and J.W.F. Valle, *Neutrino oscillations refitted*, *Phys. Rev. D* **90** (2014) 093006 [[arXiv:1405.7540](https://arxiv.org/abs/1405.7540)] [[INSPIRE](#)].
- [6] F.F. Deppisch, J. Harz and M. Hirsch, *Falsifying high-scale leptogenesis at the LHC*, *Phys. Rev. Lett.* **112** (2014) 221601 [[arXiv:1312.4447](https://arxiv.org/abs/1312.4447)] [[INSPIRE](#)].
- [7] F.F. Deppisch, J. Harz, M. Hirsch, W.-C. Huang and H. Päs, *Falsifying high-scale baryogenesis with neutrinoless double beta decay and lepton flavor violation*, *Phys. Rev. D* **92** (2015) 036005 [[arXiv:1503.04825](https://arxiv.org/abs/1503.04825)] [[INSPIRE](#)].
- [8] P.S. Bhupal Dev, C.H. Lee and R.N. Mohapatra, *TeV scale lepton number violation and baryogenesis*, *J. Phys. Conf. Ser.* **631** (2015) 012007.
- [9] S. Weinberg, *Baryon and lepton nonconserving processes*, *Phys. Rev. Lett.* **43** (1979) 1566 [[INSPIRE](#)].
- [10] T. Yanagida, *Horizontal symmetry and masses of neutrinos*, in the proceedings of the *Workshop on unified theory and baryon number in the universe*, O. Sawada and A. Sugamoto eds., KEK, Tsukuba, Japan (1979) [*Conf. Proc.* **C7902131** (1979) 95] [[INSPIRE](#)].
- [11] M. Gell-Mann, P. Ramond, R. Slansky, *Complex spinors and unified theories*, in *Supergravity*, D.Z. Freedman and P. van Nieuwenhuizen eds., North Holland, Amsterdam, The Netherlands (1979) [[INSPIRE](#)].
- [12] R. Foot, H. Lew, X.G. He and G.C. Joshi, *Seesaw neutrino masses induced by a triplet of leptons*, *Z. Phys. C* **44** (1989) 441 [[INSPIRE](#)].
- [13] R.N. Mohapatra and G. Senjanović, *Neutrino mass and spontaneous parity violation*, *Phys. Rev. Lett.* **44** (1980) 912 [[INSPIRE](#)].
- [14] E. Ma, *Pathways to naturally small neutrino masses*, *Phys. Rev. Lett.* **81** (1998) 1171 [[hep-ph/9805219](https://arxiv.org/abs/hep-ph/9805219)].
- [15] K.S. Babu and C.N. Leung, *Classification of effective neutrino mass operators*, *Nucl. Phys. B* **619** (2001) 667 [[hep-ph/0106054](https://arxiv.org/abs/hep-ph/0106054)] [[INSPIRE](#)].
- [16] G.F. Giudice and O. Lebedev, *Higgs-dependent Yukawa couplings*, *Phys. Lett. B* **665** (2008) 79 [[arXiv:0804.1753](https://arxiv.org/abs/0804.1753)] [[INSPIRE](#)].
- [17] K.S. Babu, S. Nandi and Z. Tavartkiladze, *New mechanism for neutrino mass generation and triply charged Higgs bosons at the LHC*, *Phys. Rev. D* **80** (2009) 071702 [[arXiv:0905.2710](https://arxiv.org/abs/0905.2710)] [[INSPIRE](#)].

- [18] F. Bonnet, D. Hernandez, T. Ota and W. Winter, *Neutrino masses from higher than  $D = 5$  effective operators*, *JHEP* **10** (2009) 076 [[arXiv:0907.3143](#)] [[INSPIRE](#)].
- [19] I. Picek and B. Radovic, *Novel TeV-scale seesaw mechanism with Dirac mediators*, *Phys. Lett. B* **687** (2010) 338 [[arXiv:0911.1374](#)] [[INSPIRE](#)].
- [20] S. Kanemura and T. Ota, *Neutrino masses from loop-induced  $d \geq 7$  operators*, *Phys. Lett. B* **694** (2011) 233 [[arXiv:1009.3845](#)] [[INSPIRE](#)].
- [21] M.B. Krauss, T. Ota, W. Porod and W. Winter, *Neutrino mass from higher than  $D = 5$  effective operators in SUSY and its test at the LHC*, *Phys. Rev. D* **84** (2011) 115023 [[arXiv:1109.4636](#)] [[INSPIRE](#)].
- [22] M.B. Krauss, D. Meloni, W. Porod and W. Winter, *Neutrino mass from a  $D = 7$  effective operator in an SU(5) SUSY-GUT framework*, *JHEP* **05** (2013) 121 [[arXiv:1301.4221](#)] [[INSPIRE](#)].
- [23] G. Bambhaniya, J. Chakraborty, S. Goswami and P. Konar, *Generation of neutrino mass from new physics at TeV scale and multilepton signatures at the LHC*, *Phys. Rev. D* **88** (2013) 075006 [[arXiv:1305.2795](#)] [[INSPIRE](#)].
- [24] H. Pas, M. Hirsch, H.V. Klapdor-Kleingrothaus and S.G. Kovalenko, *Towards a superformula for neutrinoless double beta decay*, *Phys. Lett. B* **453** (1999) 194 [[INSPIRE](#)].
- [25] H. Pas, M. Hirsch, H.V. Klapdor-Kleingrothaus and S.G. Kovalenko, *A superformula for neutrinoless double beta decay. 2. The short range part*, *Phys. Lett. B* **498** (2001) 35 [[hep-ph/0008182](#)] [[INSPIRE](#)].
- [26] F. Bonnet, M. Hirsch, T. Ota and W. Winter, *Systematic decomposition of the neutrinoless double beta decay operator*, *JHEP* **03** (2013) 055 [Erratum *ibid.* **04** (2014) 090] [[arXiv:1212.3045](#)] [[INSPIRE](#)].
- [27] J.C. Helo, M. Hirsch, T. Ota and F.A. P.d. Santos, *Double beta decay and neutrino mass models*, *JHEP* **05** (2015) 092 [[arXiv:1502.05188](#)] [[INSPIRE](#)].
- [28] A. de Gouvêa and J. Jenkins, *A survey of lepton number violation via effective operators*, *Phys. Rev. D* **77** (2008) 013008 [[arXiv:0708.1344](#)] [[INSPIRE](#)].
- [29] P.W. Angel, N.L. Rodd and R.R. Volkas, *Origin of neutrino masses at the LHC:  $\Delta L = 2$  effective operators and their ultraviolet completions*, *Phys. Rev. D* **87** (2013) 073007 [[arXiv:1212.6111](#)] [[INSPIRE](#)].
- [30] P.W. Angel, Y. Cai, N.L. Rodd, M.A. Schmidt and R.R. Volkas, *Testable two-loop radiative neutrino mass model based on an  $LLQd^c Qd^c$  effective operator*, *JHEP* **10** (2013) 118 [Erratum *ibid.* **11** (2014) 092] [[arXiv:1308.0463](#)] [[INSPIRE](#)].
- [31] J.C. Helo, M. Hirsch, H. Päs and S.G. Kovalenko, *Short-range mechanisms of neutrinoless double beta decay at the LHC*, *Phys. Rev. D* **88** (2013) 073011 [[arXiv:1307.4849](#)] [[INSPIRE](#)].
- [32] J.C. Helo and M. Hirsch, *LHC dijet constraints on double beta decay*, *Phys. Rev. D* **92** (2015) 073017 [[arXiv:1509.00423](#)] [[INSPIRE](#)].
- [33] P.S.B. Dev, D. Kim and R.N. Mohapatra, *Disambiguating seesaw models using invariant mass variables at hadron colliders*, *JHEP* **01** (2016) 118 [[arXiv:1510.04328](#)] [[INSPIRE](#)].
- [34] K.S. Babu and R.N. Mohapatra, *New vector-scalar contributions to neutrinoless double beta decay and constraints on R-parity violation*, *Phys. Rev. Lett.* **75** (1995) 2276 [[hep-ph/9506354](#)] [[INSPIRE](#)].
- [35] H. Pas, M. Hirsch and H.V. Klapdor-Kleingrothaus, *Improved bounds on SUSY accompanied neutrinoless double beta decay*, *Phys. Lett. B* **459** (1999) 450 [[hep-ph/9810382](#)] [[INSPIRE](#)].



- [36] M. Hirsch, H.V. Klapdor-Kleingrothaus and S.G. Kovalenko, *New leptoquark mechanism of neutrinoless double beta decay*, *Phys. Rev. D* **54** (1996) 4207 [[hep-ph/9603213](#)] [[INSPIRE](#)].
- [37] J.C. Pati and A. Salam, *Lepton number as the fourth color*, *Phys. Rev. D* **10** (1974) 275 [*Erratum ibid.* **D 11** (1975) 703] [[INSPIRE](#)].
- [38] R.N. Mohapatra and J.C. Pati, *A natural left-right symmetry*, *Phys. Rev. D* **11** (1975) 2558 [[INSPIRE](#)].
- [39] R.N. Mohapatra and G. Senjanović, *Neutrino masses and mixings in gauge models with spontaneous parity violation*, *Phys. Rev. D* **23** (1981) 165 [[INSPIRE](#)].
- [40] Y. Cai, J.D. Clarke, M.A. Schmidt and R.R. Volkas, *Testing radiative neutrino mass models at the LHC*, *JHEP* **02** (2015) 161 [[arXiv:1410.0689](#)] [[INSPIRE](#)].
- [41] L. Lehman, *Extending the standard model effective field theory with the complete set of dimension-7 operators*, *Phys. Rev. D* **90** (2014) 125023 [[arXiv:1410.4193](#)] [[INSPIRE](#)].
- [42] S. Bhattacharya and J. Wudka, *Dimension seven operators in standard model with right handed neutrinos*, [arXiv:1505.05264](#) [[INSPIRE](#)].
- [43] N. Mahajan, *Neutrinoless double- $\beta$  decay and QCD corrections*, *Phys. Rev. Lett.* **112** (2014) 031804.
- [44] M. González, M. Hirsch and S.G. Kovalenko, *QCD running in neutrinoless double beta decay: short-range mechanisms*, *Phys. Rev. D* **93** (2016) 013017 [[arXiv:1511.03945](#)] [[INSPIRE](#)].
- [45] T. Peng, M.J. Ramsey-Musolf and P. Winslow, *TeV lepton number violation: from neutrinoless double- $\beta$  decay to the LHC*, *Phys. Rev. D* **93** (2016) 093002 [[arXiv:1508.04444](#)] [[INSPIRE](#)].
- [46] KAMLAND-ZEN collaboration, A. Gando et al., *Limit on neutrinoless  $\beta\beta$  decay of  $^{136}\text{Xe}$  from the first phase of KamLAND-Zen and comparison with the positive claim in  $^{76}\text{Ge}$* , *Phys. Rev. Lett.* **110** (2013) 062502 [[arXiv:1211.3863](#)] [[INSPIRE](#)].
- [47] Y. Koide, *Can the Zee model explain the observed neutrino data?*, *Phys. Rev. D* **64** (2001) 077301 [[hep-ph/0104226](#)] [[INSPIRE](#)].
- [48] K.S. Babu and J. Julio, *Radiative neutrino mass generation through vector-like quarks*, *Phys. Rev. D* **85** (2012) 073005 [[arXiv:1112.5452](#)] [[INSPIRE](#)].
- [49] W.C. Haxton and G.J. Stephenson, *Double beta decay*, *Prog. Part. Nucl. Phys.* **12** (1984) 409 [[INSPIRE](#)].
- [50] K. Muto, E. Bender and H.V. Klapdor, *Nuclear structure effects on the neutrinoless double beta decay*, *Z. Phys. A* **334** (1989) 187 [[INSPIRE](#)].
- [51] S. Antusch, C. Biggio, E. Fernandez-Martinez, M.B. Gavela and J. Lopez-Pavon, *Unitarity of the leptonic mixing matrix*, *JHEP* **10** (2006) 084 [[hep-ph/0607020](#)] [[INSPIRE](#)].
- [52] E. Akhmedov, A. Kartavtsev, M. Lindner, L. Michaels and J. Smirnov, *Improving electro-weak fits with TeV-scale sterile neutrinos*, *JHEP* **05** (2013) 081 [[arXiv:1302.1872](#)] [[INSPIRE](#)].
- [53] S. Antusch and O. Fischer, *Non-unitarity of the leptonic mixing matrix: Present bounds and future sensitivities*, *JHEP* **10** (2014) 094 [[arXiv:1407.6607](#)] [[INSPIRE](#)].
- [54] F.J. Escrihuela, D.V. Forero, O.G. Miranda, M. Tortola and J.W.F. Valle, *On the description of non-unitary neutrino mixing*, *Phys. Rev. D* **92** (2015) 053009 [[arXiv:1503.08879](#)] [[INSPIRE](#)].

- [55] F. del Aguila, A. Aparici, S. Bhattacharya, A. Santamaria and J. Wudka, *Effective lagrangian approach to neutrinoless double beta decay and neutrino masses*, *JHEP* **06** (2012) 146 [[arXiv:1204.5986](#)] [[INSPIRE](#)].
- [56] F. Bonnet, M. Hirsch, T. Ota and W. Winter, *Systematic study of the  $D = 5$  Weinberg operator at one-loop order*, *JHEP* **07** (2012) 153 [[arXiv:1204.5862](#)] [[INSPIRE](#)].
- [57] M. Hirsch, H.V. Klapdor-Kleingrothaus and S.G. Kovalenko, *New low-energy leptoquark interactions*, *Phys. Lett. B* **378** (1996) 17 [[hep-ph/9602305](#)] [[INSPIRE](#)].
- [58] D. Aristizabal Sierra, M. Hirsch and S.G. Kovalenko, *Leptoquarks: Neutrino masses and accelerator phenomenology*, *Phys. Rev. D* **77** (2008) 055011 [[arXiv:0710.5699](#)] [[INSPIRE](#)].
- [59] J. Stupak III, *Search for 1st-generation leptoquarks using the ATLAS detector*, *EPJ Web Conf.* **28** (2012) 12012 [[arXiv:1202.1369](#)] [[INSPIRE](#)].
- [60] ATLAS collaboration, *Search for second generation scalar leptoquarks in  $pp$  collisions at  $\sqrt{s} = 7$  TeV with the ATLAS detector*, *Eur. Phys. J. C* **72** (2012) 2151 [[arXiv:1203.3172](#)] [[INSPIRE](#)].
- [61] CMS collaboration, *Search for pair-production of first generation scalar leptoquarks in  $pp$  collisions at  $\sqrt{s} = 8$  TeV*, *CMS-PAS-EXO-12-041* (2012).
- [62] CMS collaboration, *Search for third-generation scalar leptoquarks in the  $t\tau$  channel in proton-proton collisions at  $\sqrt{s} = 8$  TeV*, *JHEP* **07** (2015) 042 [[arXiv:1503.09049](#)] [[INSPIRE](#)].
- [63] CMS collaboration, *Search for pair production of third-generation scalar leptoquarks and top squarks in proton-proton collisions at  $\sqrt{s} = 8$  TeV*, *Phys. Lett. B* **739** (2014) 229 [[arXiv:1408.0806](#)] [[INSPIRE](#)].
- [64] D. Aristizabal Sierra, A. Degee, L. Dorame and M. Hirsch, *Systematic classification of two-loop realizations of the Weinberg operator*, *JHEP* **03** (2015) 040 [[arXiv:1411.7038](#)] [[INSPIRE](#)].
- [65] L. Lavoura, *General formulae for  $f_1 \rightarrow f_2\gamma$* , *Eur. Phys. J. C* **29** (2003) 191 [[hep-ph/0302221](#)] [[INSPIRE](#)].
- [66] SUPERNEMO collaboration, R. Arnold et al., *Probing new physics models of neutrinoless double beta decay with SuperNEMO*, *Eur. Phys. J. C* **70** (2010) 927 [[arXiv:1005.1241](#)] [[INSPIRE](#)].
- [67] J.A. Casas and A. Ibarra, *Oscillating neutrinos and  $\mu\text{on} \rightarrow e, \gamma$* , *Nucl. Phys. B* **618** (2001) 171 [[hep-ph/0103065](#)] [[INSPIRE](#)].
- [68] MEG collaboration, J. Adam et al., *New constraint on the existence of the  $\mu^+ \rightarrow e^+\gamma$  decay*, *Phys. Rev. Lett.* **110** (2013) 201801 [[arXiv:1303.0754](#)] [[INSPIRE](#)].
- [69] M. Doi, T. Kotani and E. Takasugi, *Double beta decay and Majorana neutrino*, *Prog. Theor. Phys. Suppl.* **83** (1985) 1 [[INSPIRE](#)].
- [70] J. Barry and W. Rodejohann, *Lepton number and flavour violation in TeV-scale left-right symmetric theories with large left-right mixing*, *JHEP* **09** (2013) 153 [[arXiv:1303.6324](#)] [[INSPIRE](#)].
- [71] P.S. Bhupal Dev, S. Goswami and M. Mitra, *TeV scale left-right symmetry and large mixing effects in neutrinoless double beta decay*, *Phys. Rev. D* **91** (2015) 113004 [[arXiv:1405.1399](#)] [[INSPIRE](#)].
- [72] PARTICLE DATA GROUP, J. Beringer et al., *Review of particle physics*, *Phys. Rev. D* **86** (2012) 010001 [[INSPIRE](#)].

- [73] CMS collaboration, *Search for heavy neutrinos and W bosons with right-handed couplings in proton-proton collisions at  $\sqrt{s} = 8$  TeV*, *Eur. Phys. J. C* **74** (2014) 3149 [[arXiv:1407.3683](#)] [[INSPIRE](#)].
- [74] ATLAS collaboration, *Search for heavy Majorana neutrinos with the ATLAS detector in pp collisions at  $\sqrt{s} = 8$  TeV*, *JHEP* **07** (2015) 162 [[arXiv:1506.06020](#)] [[INSPIRE](#)].
- [75] K.S. Babu and J. Julio, *Two-loop neutrino mass generation through leptoquarks*, *Nucl. Phys. B* **841** (2010) 130 [[arXiv:1006.1092](#)] [[INSPIRE](#)].